ANL/CSE-13/30

Dissolution of Zirconium-Bonded, Monolithic, Uranium-Molybdenum Fuel for Uranium Recovery

Chemical Science and Engineering Division

About Argonne National Laboratory
Argonne is a U.S. Department of Energy laboratory managed by UChicago Argonne, LLC under contract DE-AC02-06CH11357. The Laboratory's main facility is outside Chicago, at 9700 South Cass Avenue, Argonne, Illinois 60439. For information about Argonne and its pioneering science and technology programs, see www.anl.gov.

DOCUMENT AVAILABILITY

Online Access: U.S. Department of Energy (DOE) reports produced after 1991 and a growing number of pre-1991 documents are available free via DOE's SciTech Connect (http://www.osti.gov/scitech/)

Reports not in digital format may be purchased by the public from the National Technical Information Service (NTIS):
U.S. Department of Commerce
National Technical Information Service
5301 Shawnee Rd
Alexandra, VA 22312
www.ntis.gov
Phone: (800) 553-NTIS (6847) or (703) 605-6000
Fax: (703) 605-6900
Email: **orders@ntis.gov**

Reports not in digital format are available to DOE and DOE contractors from the Office of Scientific and Technical Information (OSTI):
U.S. Department of Energy
Office of Scientific and Technical Information
P.O. Box 62
Oak Ridge, TN 37831-0062
www.osti.gov
Phone: (865) 576-8401
Fax: (865) 576-5728
Email: **reports@osti.gov**

Disclaimer
This report was prepared as an account of work sponsored by an agency of the United States Government. Neither the United States Government nor any agency thereof, nor UChicago Argonne, LLC, nor any of their employees or officers, makes any warranty, express or implied, or assumes any legal liability or responsibility for the accuracy, completeness, or usefulness of any information, apparatus, product, or process disclosed, or represents that its use would not infringe privately owned rights. Reference herein to any specific commercial product, process, or service by trade name, trademark, manufacturer, or otherwise, does not necessarily constitute or imply its endorsement, recommendation, or favoring by the United States Government or any agency thereof. The views and opinions of document authors expressed herein do not necessarily state or reflect those of the United States Government or any agency thereof, Argonne National Laboratory, or UChicago Argonne, LLC.

ANL/CSE-13/30

Dissolution of Zirconium-Bonded, Monolithic, Uranium-Molybdenum Fuel for Uranium Recovery

by
James Jerden, Jeffrey Fortner, and Dominique Stepinski
Chemical Science and Engineering Division, Argonne National Laboratory

prepared for
U.S. Department of Energy, National Nuclear Security Administration,
Office of Defense Nuclear Nonproliferation

May 31, 2009

CONTENTS

SCOPE AND PURPOSE 1

SUMMARY 2

1 INTRODUCTION 4

2 FUEL FABRICATION AND FORMATION OF POTENTIALLY EXPLOSIVE INTERMETALLIC PHASE 5

3 MECHANISM OF EXPLOSIVE REACTION OF INTERMETALLIC PHASE IN AIR AND NITRIC ACID 7

4 ENERGY RELEASE FROM RAPID OXIDATION OF UZr_2 10

5 MITIGATION OF THE EXPLOSIVE HAZARD POSED BY DISSOLVING Zr-BONDED U-Mo FUEL 12

6 DISSOLUTION SCENARIOS FOR ZIRCONIUM BONDED SPENT AND SCRAP U-Mo FUELS 13

7 DISSOLUTION RATES OF URANIUM-MOLYBDENUM FUEL 18

8 CHEMICAL SPECIATION OF DISSOLVER SOLUTIONS 19

8.1 Model Scenario Scrap (a) 19
8.2 Model Scenario Scrap (b) 22
8.3 Model Scenario Scrap (b) 25
8.4 Model Scenario Spent Fuel (a) 28
8.5 Model Scenario Spent Fuel (b) 35

9 CORROSION RATE OF STAINLESS STEEL AND ZIRCONIUM IN THE DISSOLVER SOLUTIONS 37

10 CONCLUSION 41

11 REFERENCES 42

FIGURES

1 U-Zr Phase Diagram 6

2 Explosive Oxidation of UZr_2 Formed during the Early Stages of the Dissolution of a Uranium-Zirconium Alloy 8

3 X-ray Diffraction Data Showing Enrichment in Explosive Uranium-Niobium Phase during Dissolution of a Uranium-Niobium Alloy in Concentrated Nitric Acid 9

4 Solubility of Molybdenum Oxide and Hydrous Molybdenum Oxide Increases with Decreasing Temperature; Solubility of MoO_3 Reaches a Maximum at a Nitric Acid Concentration around 4 moles/L and Decreases at Lower and Higher Values; Dissolved Concentration of Uranium and Molybdenum in the Presence of UO_2MoO_4 Solid, a Mixture of UO_2MoO_4 Solid and MoO_3:$2H_2O$, and MoO_3:$2H_2O$ Alone; Solubility of MoO_3 and MoO_3:$2H_2O$ Increases in the Presence of Ferric Iron 15

5 Dissolver Speciation for the Dissolution of 20 g/L U-10Mo Scrap 20

6 Dissolver Speciation for the Dissolution of 50 g/L U-10Mo Scrap 23

7 Dissolver Speciation for the Dissolution of 75 g/L U-10Mo Scrap 26

8 Dissolver Speciation for the Dissolution of 20 g/L U-10Mo Spent Fuel 29

9 Dissolver Speciation for the Dissolution of 50 g/L U-10Mo Spent Fuel 32

10 Corrosion Rates of 304 Coupons over 1 week of Testing as a Function of Initial Total Fluorine Concentration in 8-M Nitric Acid for Various Concentrations of Added Aluminum 38

11 Corrosion Rates of 304 Coupons over 1 week of Testing as a Function of Final Free Fluorine Concentration in 8-M Nitric Acid for Various Concentration of Added Aluminum 40

TABLES

1 Dissolution Scenarios for U-10Mo Fabrication Scrap Modeled in This Report 17

2 Dissolution Scenarios for Spent U-10Mo Fuel Modeled in This Report 17

DISSOLUTION OF ZIRCONIUM-BONDED, MONOLITHIC, URANIUM-MOLYBDENUM FUEL FOR URANIUM RECOVERY

SCOPE AND PURPOSE

This report presents results from a process development study of dissolution scenarios that would facilitate the recovery of uranium from both irradiated (spent) and unirradiated (scrap) U-10Mo fuel using a tributyl-phosphate-based solvent extraction process. A specific focus of this study is to assess how metals added as diffusion/bonding barriers will influence the chemistry of the fuel dissolution process. Of particular interest are fuels containing zirconium or niobium as barrier materials, because these fuels may contain an intermetallic uranium-zirconium or uranium-niobium phase (formed during fabrication and enhanced during irradiation) that could react with explosive violence during oxidative dissolution. The first part of this report will evaluate the explosive potential of this intermetallic phase and discuss means to inhibit explosive reactions in the dissolver when it is present (e.g., by the addition of fluoride to the dissolver solution). The second part of the report will discuss dissolution scenarios for both spent and scrap U-10Mo fuel and will discuss the possibility of dissolver corrosion in the fluoride bearing dissolver solutions.

SUMMARY

- A potentially explosive uranium-zirconium or uranium-niobium intermetallic phase will be present in U-10Mo fuels fabricated with zirconium or niobium bonding layers. This intermetallic phase forms during fabrication and may grow during irradiation.

- The amount of the energy that is instantaneously released during oxidative dissolution of the intermetallic phase in nitric acid is such that even a small quantity (e.g., a surface coating on a 5-g alloy sample) is enough to eject 75 mL of acid from a vessel and shatter heavy glassware (see Figure 2). Therefore, the dissolution of U-10Mo scrap and spent fuel will require the addition of fluoride to mitigate the explosive hazard posed by the intermetallic phase. A fluoride to zirconium atomic ratio of 4:1 has been shown to inhibit the explosive reaction in nitric acid in the absence of other complexing species.

- Based on solubility limits for uranium and molybdenum solids in a nitric acid, a number of dissolution scenarios for U-10Mo scrap and fuels have been developed (Stepinski et al. 2008). In this report, three of the scrap dissolution scenarios were modeled and two of the irradiated fuel dissolution scenarios were modeled. The modeling involved thermodynamic calculations that predict the speciation and saturation state with respect to potential precipitates for conditions of interest (3 moles/L HNO_3 with varying initial concentrations of HF).

- The models predict that initial HF concentrations of 0.07 moles/L and 0.2 moles/L are needed to dissolve 20 g/L U and 50 g/L of U-10Mo scrap, respectively, while maintaining a 4/1 free F-to-Zr ratio to mitigate the explosive hazard posed by the intermetallic phase. The final free fluoride concentrations (after complete dissolution) for these dissolution scenarios are 3.7×10^{-3} moles/L for 20 g/L U and 2.6×10^{-3} moles/L for 50 g/L U. The key species present for these dissolution scenarios, which assume the Al cladding has been removed prior to dissolution, are ZrF^{3+}, ZrF_3^{+}, UO_2F^{+}, and FeF_2^{+}. The models also predict that the dissolver solution will be saturated with respect to a zirconium fluoride solid if an initial HF concentration of 0.5 moles/L is used.

- The models predict that initial HF concentrations of 0.6 moles/L and 1.5 moles/L are needed to dissolve 20 g/L U and 50 g/L of irradiated U-10Mo fuel, respectively, while maintaining enough free fluoride to mitigate the explosive hazard posed by the intermetallic phase. These values are higher than the HF needed for the scrap dissolutions, because it is assumed that the aluminum cladding is not removed prior to dissolution. The final free fluoride concentrations (after complete dissolution) for these dissolution scenarios are

3.1×10^{-3} moles/L for 20 g/L U and 2.2×10^{-4} moles/L for 50 g/L U (free fluoride for 50 g/L U case is predicted to be controlled by the solubility of lanthanide fluorides). The key species present for these dissolution scenarios (which assume the Al cladding has not been removed prior to dissolution) are AlF^{2+}, ZrF^{3+}, ZrF_3^{+}, UO_2F^{+}, and FeF_2^{+}. The models also predict that the dissolver solution will be saturated with respect to lanthanide fluorides at initial HF concentrations greater than 0.6 moles/L and aluminum and zirconium fluorides at initial HF concentrations greater than 0.9 moles/L.

- At the free fluoride concentrations predicted for the scrap and irradiated U-10Mo fuel dissolution scenarios discussed above, the corrosion rate of 304L stainless steel (a potential dissolver vessel material) is predicted to be less than 30 mils/year. Determination of an "acceptable" rate of vessel corrosion is an empirical task that depends upon the construction of the vessel, the expected time of contact, and the desired service life of the system, among other factors. Such a determination requires an engineering assessment that is beyond the scope of this report, although rates below 50 mils per year (mpy) are considered "low," "mild," or "adequate" in similar contexts. Generally, the expected solution conditions compare favorably with prior reprocessing of thoria fuels and Mark-42 fuels, suggesting a tenable operation to reprocess and reclaim aluminum-clad zirconium-bonded U-10Mo fuels with existing facilities.

- Steady-state free fluoride concentrations as high as 0.005 moles/L may be required to achieve favorable dissolution rates of Al cladding and 0.01 M for the Zr bonding layer (Anderson et al. 1998; Swanson 1958; Vander Wall and Whitener 1959); however, these constraints need to be quantified by experimental studies. The dissolution rate of Al cladding could be also increased by the addition of mercury.

1 INTRODUCTION

The Fuel Development program of the National Nuclear Security Agency Global Threat Reduction Initiative (GTRI) is currently engaged in the development and testing of a novel nuclear fuel that would enable conversion of high-performance research reactors (HPRRs) to low enriched uranium (LEU) fuel (Wachs et al. 2008). To offer the same performance as the high enriched fuels (HEU) currently used in HPRRs, the LEU fuel will need to have a uranium density greater than 8–9 g of uranium per cubic centimeter of fuel (Moore et al. 2008). The most promising fuel type currently under investigation is a layered, monolithic design consisting of a uranium-molybdenum alloy foil with 10 weight percent molybdenum (this fuel is referred to as U-10Mo), enclosed within a 6061 aluminum cladding (Moore et al. 2008). The uranium-molybdenum foil is separated from the aluminum cladding by a diffusion/bonding interlayer of zirconium or another metal containing silicon or niobium. This design provides a fuel meat density of approximately 16 g of uranium per cubic centimeter, making it particularly promising as a LEU alternative for HEU in research and test reactors (Moore et al. 2008).

The baseline monolithic fuel-plate design consists of U-10Mo core with a thickness ranging from 0.01 to 0.05 cm. The fuel meat is clad in Al-6061 alloy with a thickness ranging from 0.04 to 0.24 cm (sum of both sides). The cladding and the U-10Mo foil are separated by a zirconium- or silicon-based alloy that is approximately 0.0025 cm thick.

Annually, almost 5 metric tons of LEU are required for production of U-10Mo fuel targets for U.S. HPRRs. Fabrication losses are estimated at 44%; about half of that material can be recycled to the melt and the other half needs to be processed to recover uranium (Wachs et al. 2008). The spent U-10Mo fuel will reprocessed to recover the uranium using a tributyl-phosphate-based solvent extraction process (Stepinski et al. 2008). The first step in developing a uranium recovery/reprocessing strategy involves designing and optimizing a process for dissolving the spent fuel and scrap.

This report will present thermodynamic models for some of some dissolution scenarios for the U-10Mo fuel similar to ones discussed in Stepinski et al. (2008). Particular emphasis will be placed on dissolving fuel plates that contain a zirconium or niobium diffusion/bonding interlayer between the uranium-molybdenum foil and the aluminum cladding. Previous work has shown that, under certain conditions, uranium and zirconium or uranium and niobium metals can interact (through diffusion) to form an intermetallic phase that can oxidize with explosive violence in nitric acid (e.g., Larsen et al. 1954; Gens 1958; Swanson 1959; Jackson and Johns 1970). The explosive potential of this intermetallic phase and the means to mitigate the explosive hazard during dissolution will be discussed.

2 FUEL FABRICATION AND FORMATION OF POTENTIALLY EXPLOSIVE INTERMETALLIC PHASE

The potentially explosive intermetallic phase is formed between the uranium-molybdenum fuel and the zirconium or niobium bonding layer during the fuel fabrication process. In general, the fabrication process as described by Moore et al. (2008) involves (1) producing rectangular coupons of U-10Mo by arch melting and casting; (2) laminating the coupons with the diffusion/bonding barrier (e.g., Zr, Nb, Si); (3) heating the laminated coupons at 650–700°C for 45 to 60 minutes and then hot rolling them (the coupons are "canned" in a sealed, inert atmosphere steel frame for this step, and step 3 is repeated until the desired foil thickness is achieved); (4) placing the foil back in a furnace (after rolling is complete) and heating at 675°C for 30–120 minutes to ensure ductility; (5) de-canning the foils, shearing them to the desired dimensions, and wet sanding and chemically treating them (using hydrofluoric acid, nitric acid, water and ethyl alcohol) to prepare the surface for cladding and remove surface oxide; (6) bonding the cladding, made of Al 6061 sheet stock, to the fuel foil by friction bonding or hot isostatic pressing at 560°C and 100Mpa; (7) chemically cleaning the fuel plates using sodium hydroxide and nitric acid and an aluminum oxide film ("boehmite" is applied to the cladding by immersing it in deionized water for 4 hr at 185°C and 1.1 Mpa) (Moore et al. 2008).

The phase diagram for the uranium-zirconium system shown in Figure 1 indicates that the potentially explosive intermetallic uranium-zirconium phase (identified as UZr_2 in a previous work: Swanson 1959) will form when temperatures are high enough to promote diffusion yet lower than approximately 600°C. Therefore, the intermetallic phase could form during hot rolling (step 3) as the fuel cools from an initial temperature of 650–700°C, during cool down from heating during step 4, and during hot isostatic pressing (step 6).

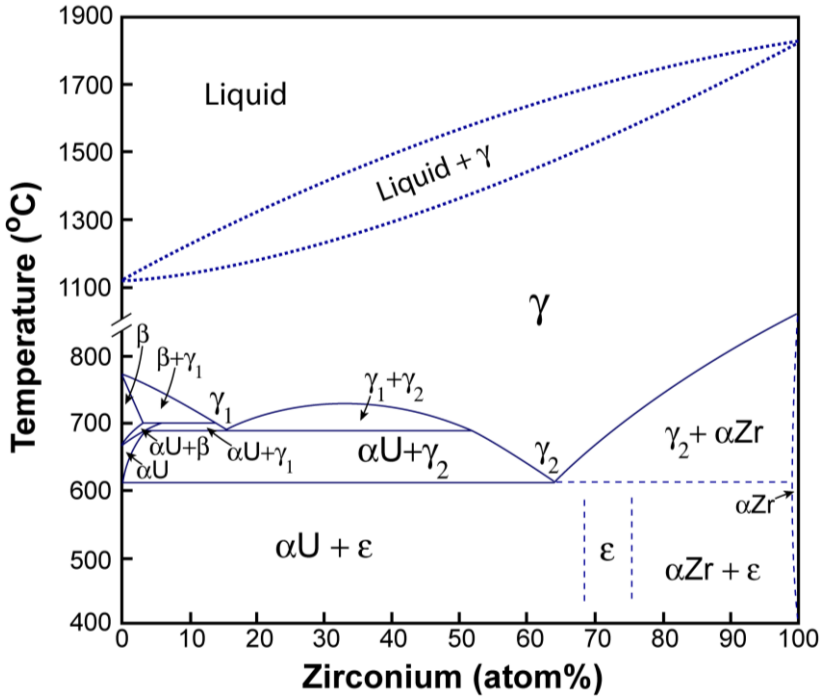

FIGURE 1 U-Zr Phase Diagram (adapted form Larsen et al. 1954) (The potentially explosive intermetallic phase [with an approximate composition UZr_2] is labeled as the ε phase on this diagram.)

3 MECHANISM OF EXPLOSIVE REACTION OF INTERMETALLIC PHASE IN AIR AND NITRIC ACID

Previous work has shown that the explosive reaction of the uranium-zirconium or uranium-niobium phase involves the nearly instantaneous oxidization of a very high surface area form (fine powder or "sponge") of the intermetallic phase (e.g., Larsen et al. 1954; Gens 1958; Swanson 1959; Jackson and Johns 1970). The high surface area of the intermetallic (identified by x-ray diffraction as UZr_2) is produced by the incongruent dissolution of the UZr_2 containing uranium alloy. For example, it has been observed that when uranium-zirconium alloys containing 1–30% zirconium are immersed in nitric acid the uranium matrix oxidizes and dissolves more rapidly than the intermetallic, thus leaving behind a finely divided residue of the intermetallic phase (described as a black powder in Larsen et al. 1954). Some of the intermetallic phase is oxidized in a non-violent manner to form a solid solution of ZrO_2-UO_2; however, the remaining finely divided residue may oxidize with explosive violence if the activation energy needed to initiate the reaction is supplied (Larsen et al. 1954) (Figure 2).

The activation energy can be overcome by a simple physical disturbance of the residue (for explosion in nitric acid) or by a spark (for explosion in air) (Larsen et al. 1954). Figure 2 shows pictures of the explosive reaction that were captured from a film titled "Explosions of Uranium-Zirconium Alloys in Nitric Acid," made by Harold Feder, Robert Larsen and Roberta Shor in 1953 (this film is referred to in Larsen et al. 1954).

Figure 2 illustrates the explosive oxidation of UZr_2 formed during the early stages of the dissolution of a uranium-zirconium alloy. The reaction involves the formation of a black powder on the surface of the metal sample within a few minutes of immersion (the black powder was confirmed to be UZr_2 by X-ray diffraction). When the UZr_2 powder was struck with a steel rod (middle images) the powder underwent nearly instantaneous oxidation. The explosive oxidation reaction was associated with a loud noise, a bright flash of visible light (white areas in the middle and right images), gas production (water vapor and NO_x) and the ejection of acid from the vessel. The images were captured from a film titled "Explosions of Uranium-Zirconium Alloys in Nitric Acid," made by Harold Feder, Robert Larsen and Roberta Shor in 1953 (Larsen et al. 1954).

The accumulation of a potentially explosive niobium-rich, uranium-niobium intermetallic is believed to be caused by the same type of process as the uranium-zirconium residue (Jackson and Johns 1970). Experiments have shown that a uranium-niobium alloy sample is preferentially dissolved, leaving behind an intermetallic phase that can oxidize with explosive violence if the activation energy needed to initiate the reaction is overcome (Jackson and Johns 1970). Figure 3 shows an example of the accumulation of a uranium-niobium intermetallic (on a monolith of consisting of 15% niobium) through the preferential attack of the uranium matrix.

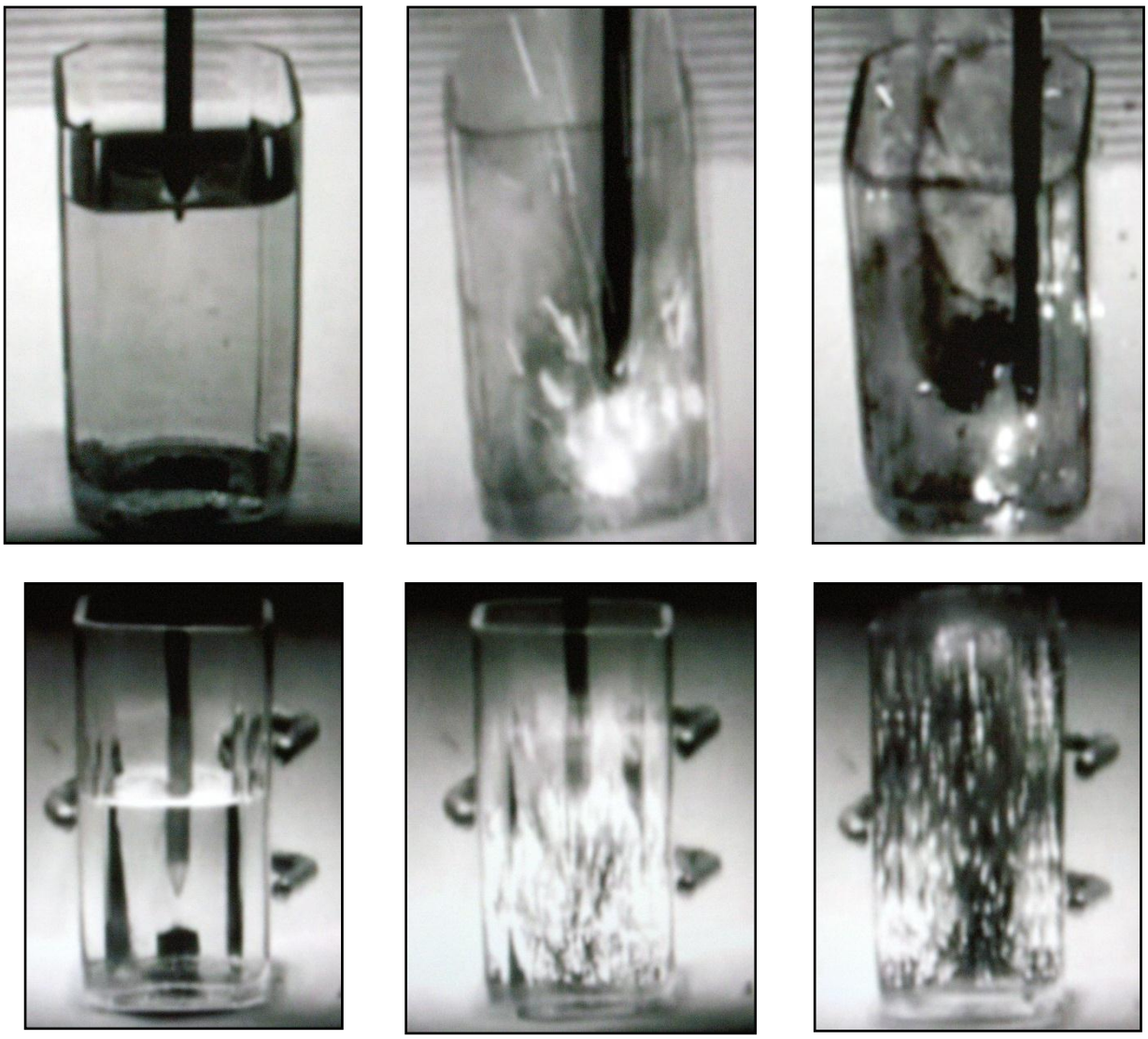

FIGURE 2 Explosive Oxidation of UZr_2 Formed during the Early Stages of the Dissolution of a Uranium-Zirconium Alloy (Top right: 5 g of U-Zr alloy [20% Zr] [black material in base of vessel] in 75-mL, 8-M nitric acid; top center: uranium-zirconium intermetallic powder accumulates on alloy surface and explodes when physically disrupted with steel rod; top right: the gas is produced from the heat of reaction [water vapor] and nitrate reduction [NO_x] is violently released; bottom left: 5 g of U-Zr alloy [2% Zr] [black material in base of vessel] in 75-mL, 16-M nitric acid; bottom center: uranium-zirconium intermetallic powder accumulates on alloy surface and explodes when disrupted with steel rod; bottom right: the gas is produced from the heat of reaction [water vapor] and nitrate reduction [NO_x] is violently released.)

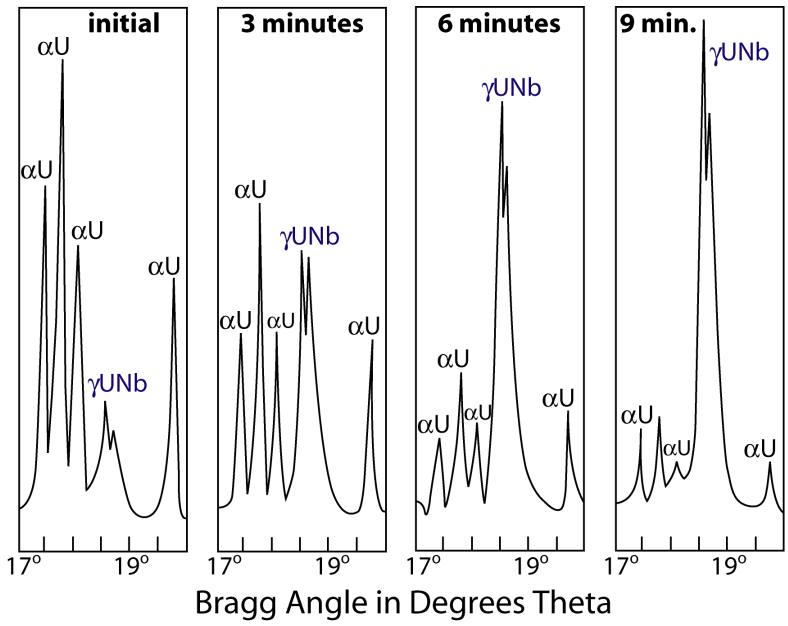

FIGURE 3 X-ray Diffraction Data (CuKα radiation) Showing Enrichment in Explosive Uranium-Niobium Phase during Dissolution of a Uranium-Niobium Alloy (15 atom% Nb) in Concentrated Nitric Acid (from Jackson and Johns 1970)

4 ENERGY RELEASE FROM RAPID OXIDATION OF UZr_2

The explosive hazard posed by the formation of a uranium-zirconium or uranium-niobium intermetallic residue during dissolution of the U-10Mo fuel depends on the amount of the intermetallic present and the amount of energy released per gram of intermetallic residue.

To estimate the amount of energy that could be released from the oxidative dissolution of the UZr_2 intermetallic phase, the enthalpy of reaction was calculated:

$$\Delta H_R^o = \sum_i n_i H_{fi}^o(\text{products}) - \sum_i n_i H_{fi}^o(\text{reactants}),$$

where n is the molar coefficient for each reactant and product from a balanced equation representing the reaction and i identifies the compounds or ions in the reaction. The standard enthalpy of formation for UZr_2 ($\Delta H_{fUZr_2}^o$) is –4kJ/mol (Nagarajan et al. 1993).

The enthalpy of reaction for the oxidative dissolution depends on what reaction products are formed:

$$UZr_2 + 10H^+ + 3.5O_2(aq) \rightarrow 5H_2O + UO_2^{2+} + 2Zr^{4+}, \quad (1)$$

$$UZr_2 + 3O_2(aq) \rightarrow UO_2(s) + 2ZrO_2(s), \quad (2)$$

$$UZr_2 + 3.5O_2(aq) + 2H_2O \rightarrow UO_3{:}H_2O + 2ZrO_2(s). \quad (3)$$

The enthalpy of reaction for reaction 1 is –3447.3 kJ/mol, for reaction; for reaction 2, it is –3282.2 kJ/mol; and for reaction 3, it is –3539.6 kJ/mol. The standard enthalpies of formation for auxiliary species ($O_2(aq)$, H_2O, UO_2^{2+}, Zr^{4+}, $UO_2(s)$, $ZrO_2(s)$ and $UO_3{:}H_2O$) are from Grenthe et al. (1992) and Brown et al. (2005).

The calculations indicate that the dissolution of UZr_2 is more exothermic than the oxidative dissolution of uranium or zirconium metals:

$$U_{metal} + 2H^+ + 1.5O_2(aq) \rightarrow H_2O + UO_2^{2+}, \quad (4)$$

$$Zr_{metal} + 4H^+ + O_2(aq) \rightarrow Zr^{4+} + 2H_2O, \quad (5)$$

where the enthalpy of reaction for reaction 4 is –1248.8 kJ/mol, and for reaction 5 it is –1080.0 kJ/mol. Similar calculations could not be made for the niobium-uranium intermetallic, due to the lack of crystallographic and thermodynamic information. However, experimental results suggest the explosive hazard posed by the uranium-niobium phase is similar in magnitude to that of the uranium-zirconium intermetallic phase (Gens 1958; Jackson and Johns 1970).

Based on the empirical observations and enthalpy calculations presented above, it is concluded that explosive oxidation of UZr_2 is caused by (1) the large enthalpy of reaction (i.e.,

the large amount of potential chemical energy in the system), and (2) the nearly instantaneous release of this energy during oxidation (as evidenced by the bright flashes of visible light emitted during oxidization: Figure 2). Empirical studies of the explosive nature of the uranium-niobium intermetallic phase suggest that its explosive nature also involves these two factors (Gens 1958; Jackson and Johns 1970). Factor 2 is associated with the physical form of the UZr_2 samples that have been observed to explode. Empirical observations (Larsen et al. 1954; Swanson 1959) suggest that the instantaneous release of energy during oxidation is due to the very high surface area (powder of sponge-like form) of the intermetallic phase. The high surface area of the intermetallic phase is imparted by the preferential dissolution of the uranium alloy matrix at a "controlled" rate. The powdery residue that is left behind (UZr_2 or uranium-niobium intermetallic) oxidizes instantaneously if a small activation energy barrier is overcome (e.g., by physically disturbing the powder).

5 MITIGATION OF THE EXPLOSIVE HAZARD POSED BY DISSOLVING Zr-BONDED U-Mo FUEL

Previous work has shown that, in the absence of other complexing species, the addition of fluoride in an atomic ratio of 4:1 fluoride to zirconium will mitigate the explosive hazard posed by dissolving a uranium-zirconium intermetallic phase (Larsen et al. 1954). The addition of fluoride inhibits the instantaneous oxidation of the intermetallic phase by "catalyzing" its dissolution through complexation. The formation of stable zirconium fluoride complexes (ZrF_4(aq), ZrF_3^+, ZrF_2^{2+}, ZrF_3^+) allows the intermetallic phase to dissolve at a "controlled" rate similar to the uranium matrix. That is, the presence of fluoride inhibits the buildup of the potentially explosive material.

6 DISSOLUTION SCENARIOS FOR ZIRCONIUM BONDED SPENT AND SCRAP U-Mo FUELS

An important consideration in designing a U-Mo fuel dissolution process is the saturation state of the dissolver solution with respect to uranium and molybdenum-bearing solids in uranyl nitrate solutions (Stepinski et al. 2008). The precipitation of uranium and molybdenum solids was observed during the processing of U-Mo alloys with 3–10 weight percent molybdenum at Hanford in low-acid feed solutions (Schulz and Duke 1959; Schulz et al. 1962). The precipitates that formed during processing were yellow and were assumed to be uranyl molybdate. The dissolved concentration of molybdenum in uranyl nitrate was observed to decrease with increased temperature and to increase with increasing nitric acid concentrations. This suggests that the solubility controlling phase (probably UO_2MoO_4) has retrograde solubility (decreasing solubility with increasing temperature) and is less stable at low pH. This precipitate from U-Mo alloy dissolution was easily centrifuged and dissolved in 0.5-M Na_2CO_3. The uranium from this secondary dissolution step was then recovered as sodium diuranate solid from the molybdate solution through the addition of sodium hydroxide (Schulz and Duke 1959; Schulz et al. 1962).

The solubilities of molybdenum solids that may precipitate during the dissolution of U-Mo fuels were studied extensively by Ferris (1961a,b) and Faugeras et al. (1961). Both studies measured the solubility of Mo(VI) oxides solids (MoO_3, and $MoO_3{:}xH_2O$) and uranyl molybdate (UO_2MoO_4) by reacting these granular samples of these minerals with nitric acid solutions over a range of acidities (under-saturation experiments). The effects of temperature and the concentrations of uranyl, ferric, and aluminum nitrate were also studied. The solids were reacted with the solutions until steady-state molybdenum concentrations were achieved. Steady state was achieved in approximately 4 hr for samples reacted at 100°C and approximately 35 days for samples reacted at 25°C (Faugeras et al. 1961).

It should be noted that, to determine solubility of a solid phase, four criteria must be met: (1) the phase must be unequivocally identified (e.g., by an x-ray or electron diffraction technique); (2) the phase must be chemically pure (e.g., not a solid solution or mixture of phases); (3) the solution aliquots used to measure the dissolved concentration of the element of interest must not contain any solids (e.g., secondary precipitates or colloids); (4) the dissolution reaction must be shown to be reversible; that is, results form under-saturation or dissolution experiments must be consistent with over-saturation or precipitation experiments (both sets of experiments should result in the same steady-state concentration of dissolved molybdenum). The results reported in Ferris (1961) and Faugeras et al. (1961) do not meet all of these criteria. For example, in some experiments containing uranyl nitrate, there appears to be a mixture of molybdenum oxide and uranyl molybdate solids. However, due to their consistency with independent experimental results, the studies by Ferris (1961) and Faugeras et al. (1961) are considered to be reliable measurements of the steady-state dissolved concentrations of molybdenum in the presence of the phases of interest (MoO_3, $MoO_3{:}xH_2O$, UO_2MoO_4).

The results from Ferris (1961a) and Faugeras et al. (1961) can be used to optimize the dissolver conditions to avoid or minimize the precipitation of molybdenum oxide and/or uranyl

molybdate during the dissolution of uranium-molybdenum fuels. Four key findings bear on this issue:

1. Molybdenum oxides and hydrous molybdenum oxides have retrograde solubility (their solubilities increase with decreasing temperature—see Figure 4a).

2. The "solubility" of molybdenum oxide at 100°C reaches a maximum (0.037 moles/L Mo) at a nitric acid concentration of 4 moles/L and decreases to less than 0.01 moles/L molybdenum at nitric acid concentrations less than 2 and greater than 8 (Figure 4b).

3. The dissolved concentrations of uranium and molybdenum in "equilibrium" with a mixture of hydrous molybdenum oxide and uranyl molybdate are 0.3 moles/L and 0.16 moles/L, respectively, at 26°C (Figure 4c). This figure also implies that uranyl molybdate solid is not stable at nitric acid concentrations greater than 3 moles/L and uranium concentrations ranging from 0.4 to 0.5 moles/L at 26°C.

4. The presence of ferric nitrate increases the solubility of hydrous molybdenum oxide (Figure 4d). This effect, presumably caused by the formation of ferric molybdate aqueous complexes (e.g., $FeMoO4^{+}$), is more pronounced at nitric acid concentrations lower than 2 moles/L.

The results from Ferris (1961a) and Faugeras et al. (1961) have been used to develop a number of scenarios for dissolving both spent U-10Mo fuel, as well as scrap uranium-molybdenum fuel fabrication (Stepinski et al. 2008). The dissolution scenarios modeled in this report are shown in Tables 1 and 2.

An important observation made in a number of studies was that the extent of dissolution of U-Mo alloys increases significantly in the presence of ferric nitrate (Schulz and Duke 1959; Ferris 1961a,b; Faugeras et al. 1961; Schulz et al. 1962). The addition of ferric nitrate allows the U-Mo alloys to be dissolved to higher terminal uranium and lower terminal acids concentrations, without re-precipitation. For example, U-10Mo can be dissolved to terminal uranium concentration of 90 g/L and 1.5-M HNO_3 without precipitate formation (Faugeras et al. 1961).

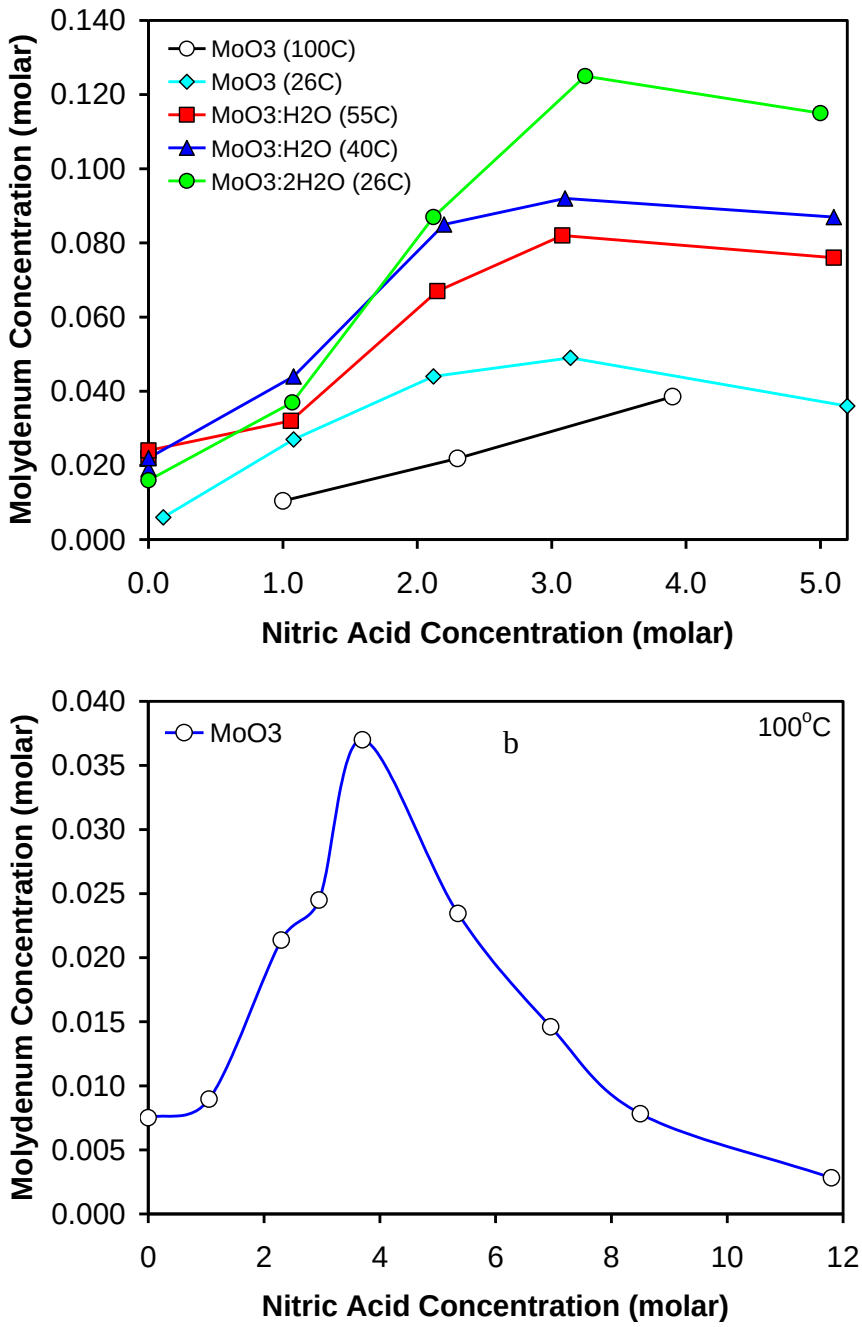

FIGURE 4 (a) Solubility of Molybdenum Oxide and Hydrous Molybdenum Oxide Increases with Decreasing Temperature (the MoO_3 data for 100°C is from Faugeras et al. [1961], all other data is from Ferris [1961a]); (b) Solubility of MoO_3 Reaches a Maximum at a Nitric Acid Concentration around 4 moles/L and Decreases at Lower and Higher Values (data from Faugeras et al. 1961); (c) Dissolved Concentration of Uranium and Molybdenum in the Presence of UO_2MoO_4 Solid, a Mixture of UO_2MoO_4 Solid and MoO_3:$2H_2O$, and MoO_3:$2H_2O$ Alone (data is from Ferris 1961a); (d) Solubility of MoO_3, and MoO_3:$2H_2O$ Increases in the Presence of Ferric Iron (added as ferric nitrate) (data is from Ferris 1961a)

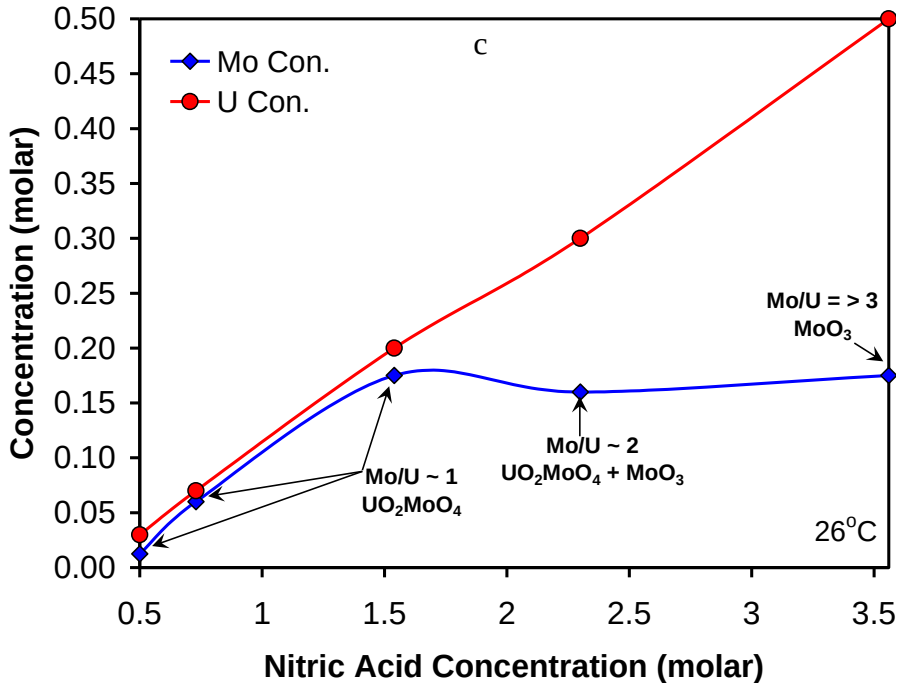

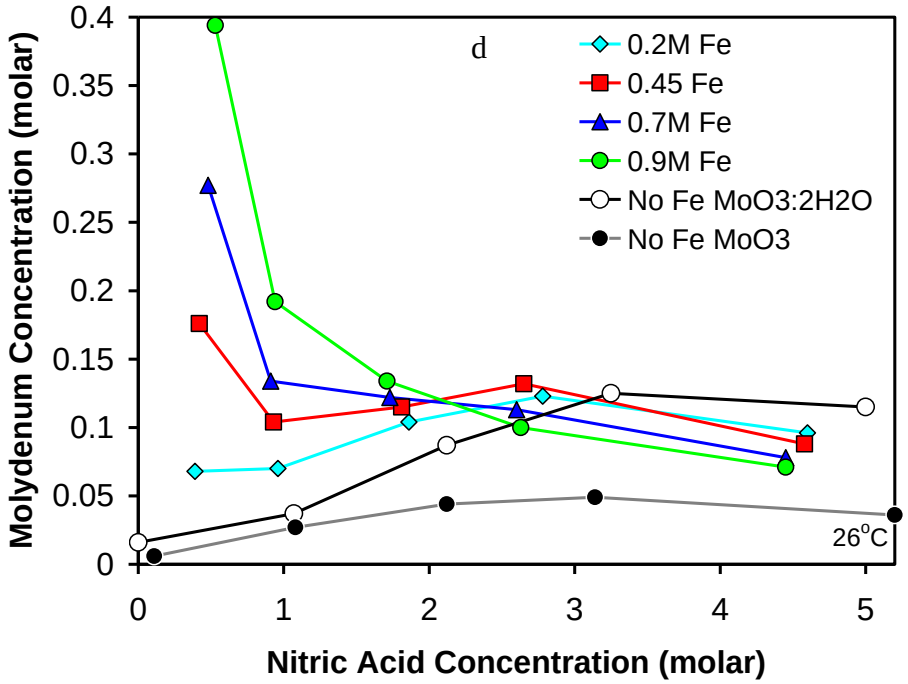

FIGURE 4 (Cont.)

TABLE 1 Dissolution Scenarios for U-10Mo Fabrication Scrap Modeled in This Report (results shown in Figures 5–7)[a]

Model Scenario	U (g/L)	Mo (g/L)	U (M)	Mo (M)	Zr (M)	Fe (M)
Scrap (a)	20.0	2.2	0.084	0.023	0.017	6.2×10^{-4}
Scrap (b)	50.0	5.6	0.21	0.058	0.042	0.5
Scrap (c)	75.0	8.3	0.32	0.087	0.063	0.5

[a] For these models, it was assumed that the Al-6061 was removed prior to dissolution. M = moles/L; Fe added as $Fe(NO_3)_3$ to dissolver solution (HNO_3 + HF) prior to dissolution.

TABLE 2 Dissolution Scenarios for Spent U-10Mo Fuel Modeled in This Report (results shown in Figures 8 and 9)[a]

Model Scenario	U (g/L)	Mo (g/L)	Al (g/L)	U (M)	Mo (M)	Al (M)	Zr (M)	Fe (M)
Fuel (a)	20.0	2.2	12.4	0.084	0.023	0.450	0.017	6.22×10^{-4}
Fuel (b)	50.0	5.6	31.0	0.210	0.058	1.12	0.042	0.5
From Al-6061	**Mg (M)**	**Si (M)**	**Cu (M)**	**Ti (M)**	**Cr (M)**	**Zn (M)**	**Mn (M)**	**V (M)**
Fuel (a)	4.69×10^{-3}	3.36×10^{-3}	4.29×10^{-4}	2.59×10^{-4}	1.67×10^{-4}	1.14×10^{-4}	9.03×10^{-5}	2.43×10^{-5}
Fuel (b)	1.17×10^{-2}	8.39×10^{-3}	1.07×10^{-3}	6.47×10^{-4}	4.17×10^{-4}	2.84×10^{-4}	2.26×10^{-4}	6.09×10^{-5}
Fission Products	**La (M)**	**Ce (M)**	**Nd (M)**	**Cs (M)**	**Sr (M)**	**Y (M)**	**Ba (M)**	**I_2 (M)**
Fuel (a)	2.29×10^{-4}	4.39×10^{-4}	7.36×10^{-4}	4.45×10^{-4}	2.83×10^{-4}	1.77×10^{-4}	2.97×10^{-4}	8.38×10^{-7}
Fuel (b)	5.72×10^{-4}	1.10×10^{-3}	1.84×10^{-3}	1.11×10^{-3}	7.06×10^{-4}	4.43×10^{-4}	7.43×10^{-4}	2.10×10^{-6}

[a] The concentrations of elements that are constituents of the Al-6061 alloy (cladding) and selected fission products that were included in the models are also shown. The fission product concentrations are for a 1.5-MW burnup uranium foil that has been cooled for 10 years (Stepinski et al. 2008). M = moles/L; Fe added as $Fe(NO_3)_3$ to dissolver solution (HNO_3 + HF) prior to dissolution

7 DISSOLUTION RATES OF URANIUM-MOLYBDENUM FUEL

The dissolution rates for U-Mo alloys in nitric acid are higher than those for uranium metal (Schulz and Duke 1959; Ferris 1961a,b; Faugeras et al. 1961; Schulz et al. 1962). The dissolution rate at the boiling temperature for U-10Mo alloy follows a third-power dependence on nitric acid concentration (Ferris 1961b). The dissolution rate is approximately 100 mg/min-cm^2 in 6-M HNO_3 and approximately 2 mg/min-cm^2 in boiling 2-M HNO_3 (Ferris 1961b). Dissolved ferric iron catalyzes the dissolution of U-Mo alloys at low acidities. For example, the dissolution rate in 1.0-M $Fe(NO_3)_3$ is about 1000 times greater than in $NaNO_3$–HNO_3 solution, given comparable acidity (pH ~0.2) and nitrate-ion concentrations (Ferris 1961b).

In the case of a one-step dissolution, where the aluminum cladding of the U-10Mo fuel will be dissolved with the uranium-molybdenum fuel meat and zirconium bonding layer, the dissolver composition must be formulated to obtain reasonable dissolution rates for the aluminum and zirconium, and to mitigate the hazard posed by the potentially explosive uranium-zirconium intermetallic phase. Previous work has shown that the addition of mercury or fluoride is required to catalyze the dissolution of the aluminum cladding (Zeyfang 1979; Bradford and Adler 1954; Anderson and Christian 1998; Crooks et al. 2003). Fluoride is also needed to ensure a satisfactory dissolution rate for the zirconium bonding layer (Vander Wall et al. 1959) and to mitigate the explosive hazard posed by the uranium-zirconium intermetallic phase (Larsen et al. 1954).

The amount of fluoride needed to dissolve the aluminum cladding within a reasonable amount of time (less than 6 hr) can be calculated based on the thickness of the aluminum plates and the measured dissolution rates. The baseline fuel-plate design consists of U-10Mo alloy foil in the 0.01–0.05 cm thickness range, a 0.0025-cm thick zirconium or silicon-based bonding layer, and Al-6061 cladding that ranges in thickness from 0.04 to 0.24 cm.

The Al-6061 cladding dissolves at a rate of 80 mg/cm^{2}hr in 7 moles/L nitric acid containing 0.02 moles/L hydrofluoric acid; the dissolution rate does not increase at higher HF concentration (Anderson and Christian 1998). At 0.005 mole/L HF the dissolution rate is 60 mg/cm^{2}hr; however, below that concentration the dissolution rate slows dramatically (Anderson and Christian 1998). The mass per area of the aluminum cladding for the U-10Mo fuels under consideration ranges from 67.5 to 324.0 mg/cm^2. Therefore, dissolution of cladding would take 1–5.4 hr, depending on the thickness of the aluminum cladding and the steady-state free fluoride concentration (the 5.4-hr dissolution time assumes 324 mg/cm^2 Al-6061 and a constant HF concentration of 0.005 moles/L).

More experimental data for the dissolution scenarios of interest (2–5 moles/L HNO_3 + <0.005 moles/L steady state free fluoride) are needed to confirm the dissolution kinetics of the U-10Mo scrap and irradiated fuel.

8 CHEMICAL SPECIATION OF DISSOLVER SOLUTIONS

The speciation of the dissolver solution for the dissolution scenarios shown in Tables 1 and 2 were modeled using the thermo-chemical modeling code OLI Systems Environmental Simulation Program. The program uses a Gibbs free energies of formation, enthalpies of formation, and heat capacities to determine the equilibrium state of the system for a set of specified conditions. The model includes the equilibrium speciation of the solution and gas phase, as well as the saturation state of the solution with respect to relevant solids (potential precipitates).

The nitric acid concentration and temperature for all dissolution scenarios discussed below are 3.0 moles/L and 25°C, respectively.

The models results are presented in Figures 5 through 9 and the conditions of each model run are described in the figure captions. The key observations from the simulations are described in the following sections.

8.1 MODEL SCENARIO SCRAP (a) (20 g/L U NO Al, TABLE 1, FIGURE 5)

- The free fluoride concentration after the dissolution ranges from 1×10^{-5} to 0.01 moles/L over an initial HF concentration range of 0.01 to 0.1 moles/L HF.

- At least 0.07 moles/L HF must be added to the dissolver solution to achieve the 4:1 F:Zr safety factor required to mitigate the explosive hazard posed by the intermetallic UZr_2 phase. This corresponds to a free fluoride concentration of 3.7×10^{-3} moles/L at the end of the dissolution.

- The dominant iron species present after dissolution is iron molybdate ($FeMoO_4^+$). The dominant zirconium species are ZrF^{3+} and ZrF_3^+, with the zirconium molybdate $ZrMoO_4^{2+}$ dominant at low initial HF concentrations. The uranyl fluoride complex UO_2F^+ becomes a dominant species at high initial HF concentrations.

Figure 5 illustrates dissolver speciation for the dissolution of 20 g/L U-10Mo scrap. Each point represents an equilibrium calculation (full dissolution of metals) for a given initial HF concentration (labeled as HF added). It is assumed that the Al cladding is removed prior to dissolution for the scrap recovery calculations. This model is for the dissolution of 0.084 moles/L U (20 g/L), 0.023 moles/L Mo, and 0.017 moles/L Zr in 3 moles/L HNO_3 containing 6×10^{-4} moles/L $Fe(NO_3)_3$ at 25°C. The same model run at 100°C showed similar results.

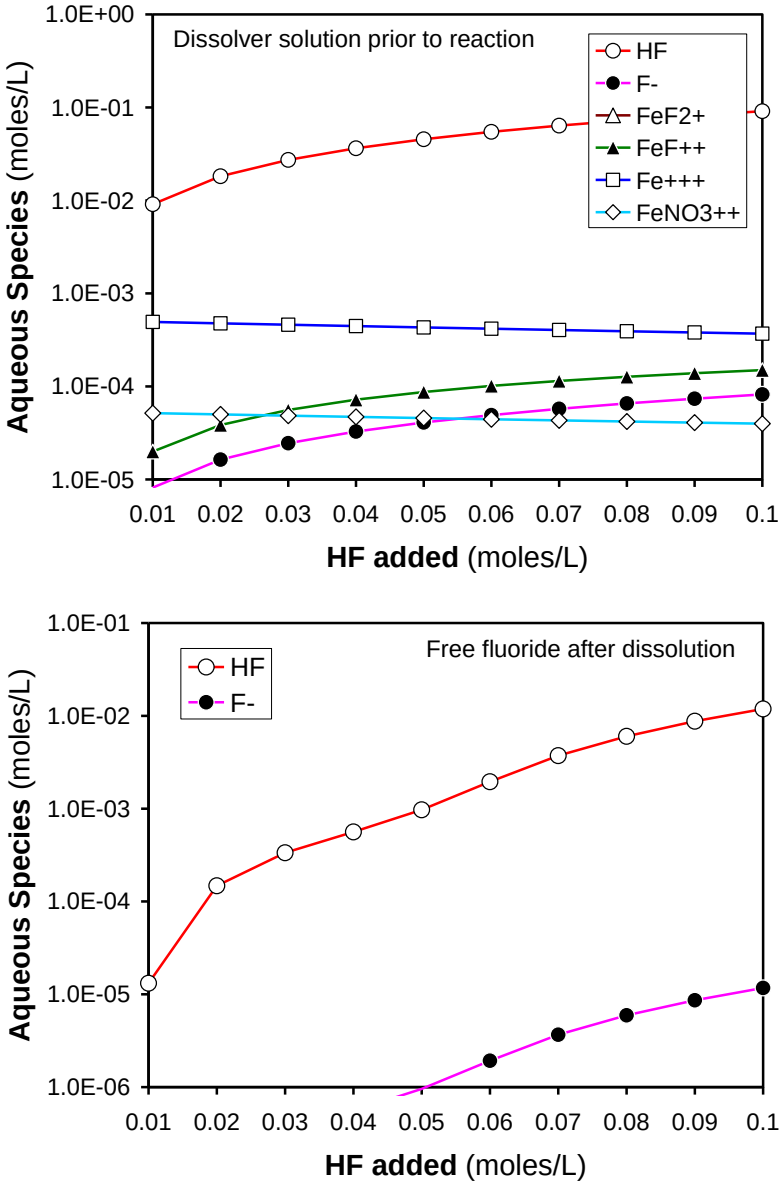

FIGURE 5 Dissolver Speciation for the Dissolution of 20 g/L U-10Mo Scrap (Top: speciation in the dissolver solution prior to reaction with metals; middle: free fluoride concentration after dissolution of metals; bottom: iron species after dissolution of metals.)

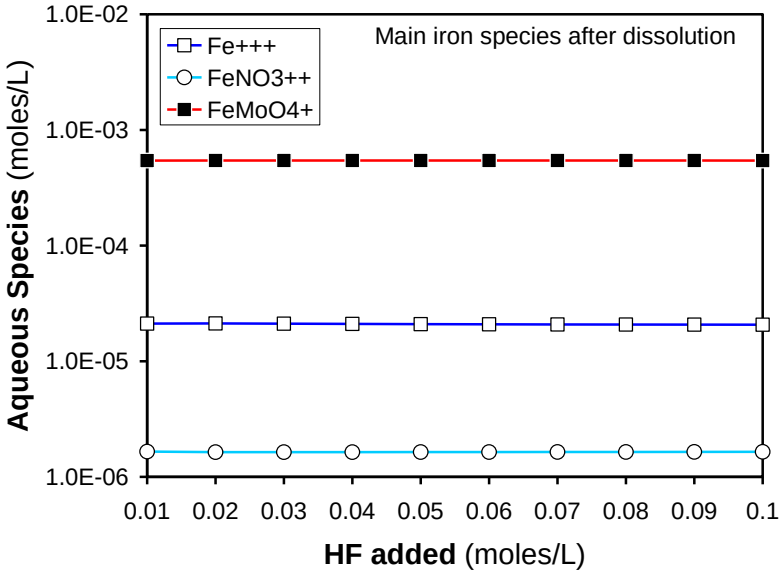

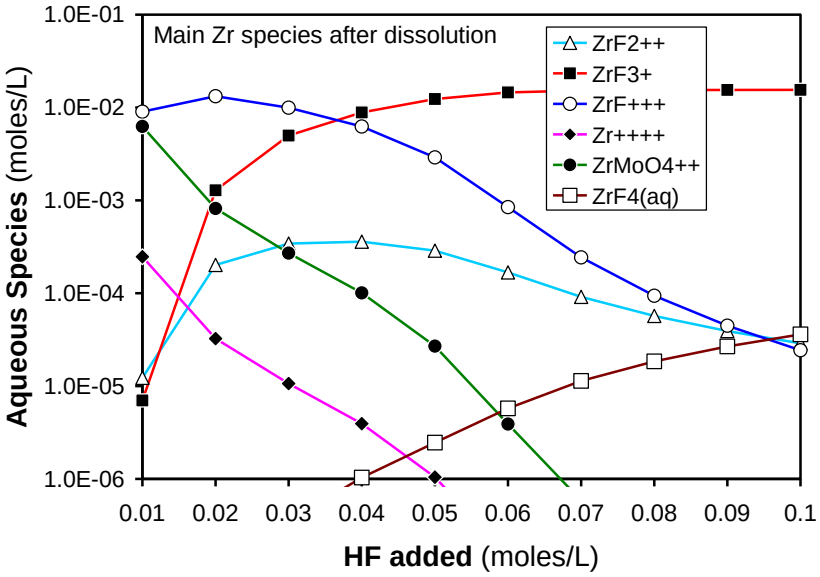

FIGURE 5 (Cont.)

(Plots show zirconium and uranium species in dissolver solution after dissolution of metals as a function of initial HF added.)

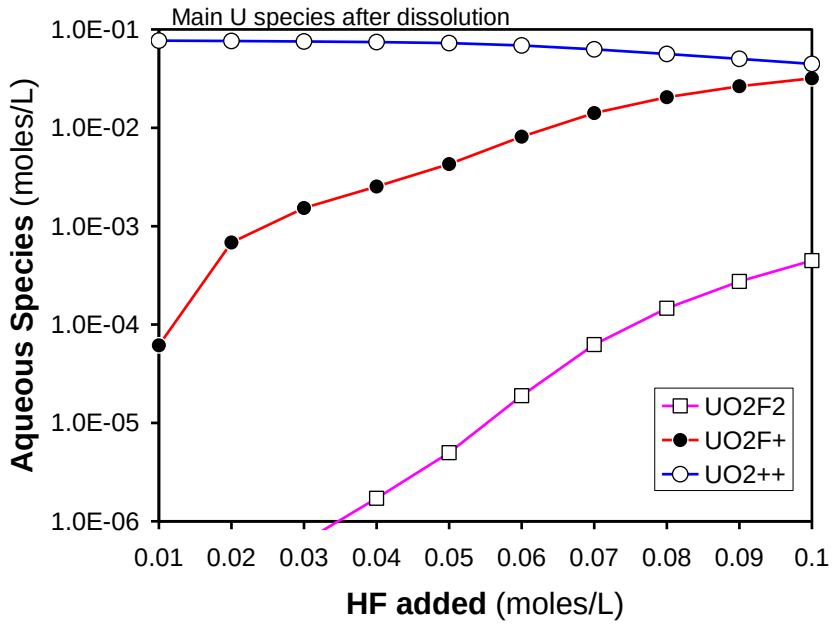

FIGURE 5 (Cont.)

8.2 MODEL SCENARIO SCRAP (b) (50 g/L U NO Al, TABLE 1, FIGURE 6)

- Prior to dissolution, the dissolver solution is dominated by iron species that form due to the presence of ferric nitrate (added to dissolver to complex molybdenum during the dissolution reaction). The dominant species are Fe^{3+}, $FeNO_3^{2+}$, and FeF_2^{+}. Thus, ferric fluoride (FeF_2^{+}) acts as a buffer of the free fluoride concentration in the dissolver solution (HNO_3+HF+$Fe(NO_3)_3$) prior to reaction with the fuel or scrap. For example, a dissolver solution consisting of 3 moles/L HNO_3, 0.4 moles/L HF, and 0.5 moles/L $Fe(NO_3)_3$ will have a free fluoride concentration of approximately 0.1 moles/L prior to the dissolution reaction (top plot in Figure 6).

- The free fluoride concentration after the dissolution ranges from 1×10^{-4} to 0.03 moles/L over an initial HF concentration range of 0.05 to 0.5 moles/L HF.

- At an initial HF concentration of 0.5 moles/L the dissolver solution is predicted to be saturated with respect to the zirconium fluoride solid ZrF_4:H_2O.

- At least 0.2 moles/L HF must be added to the dissolver solution to achieve the 4:1 F:Zr safety factor required to mitigate the explosive hazard posed by the intermetallic UZr_2 phase. This corresponds to a free fluoride concentration of 2.6×10^{-3} moles/L at the end of the dissolution.

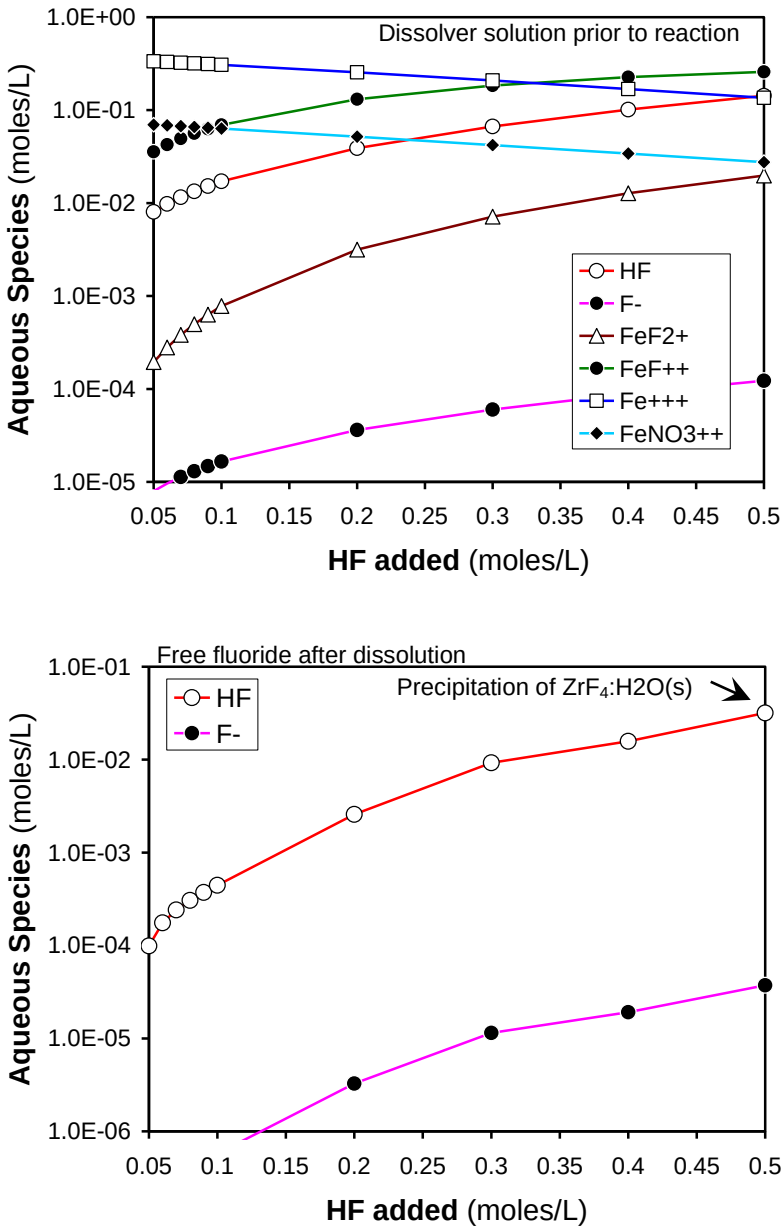

FIGURE 6 Dissolver Speciation for the Dissolution of 50 g/L U-10Mo Scrap (Top: speciation in the dissolver solution prior to reaction with metals. Middle: free fluoride concentration after dissolution of metals. Note the precipitation of a zirconium fluoride solid when the initial HF concentration is greater than 0.45 moles/L. When the model was run at 100°C the zirconium fluoride solid was not predicted to precipitate. Bottom: iron species after dissolution of metals.)

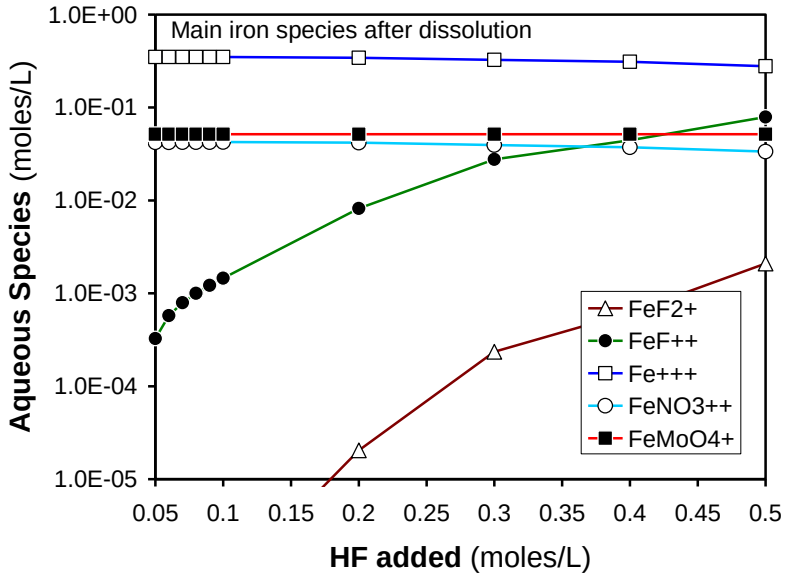

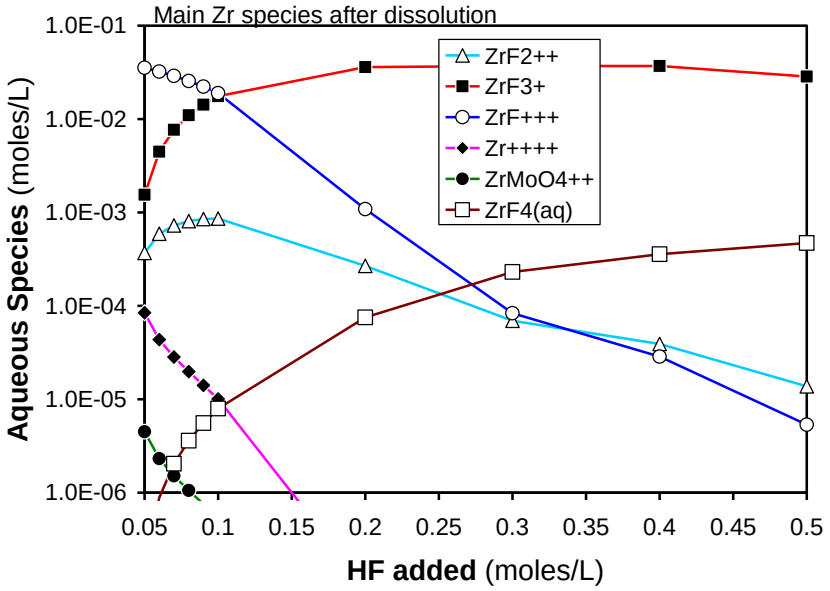

FIGURE 6 (Cont.)

(Plots show zirconium and uranium species in dissolver solution after dissolution of metals as a function of initial HF added.)

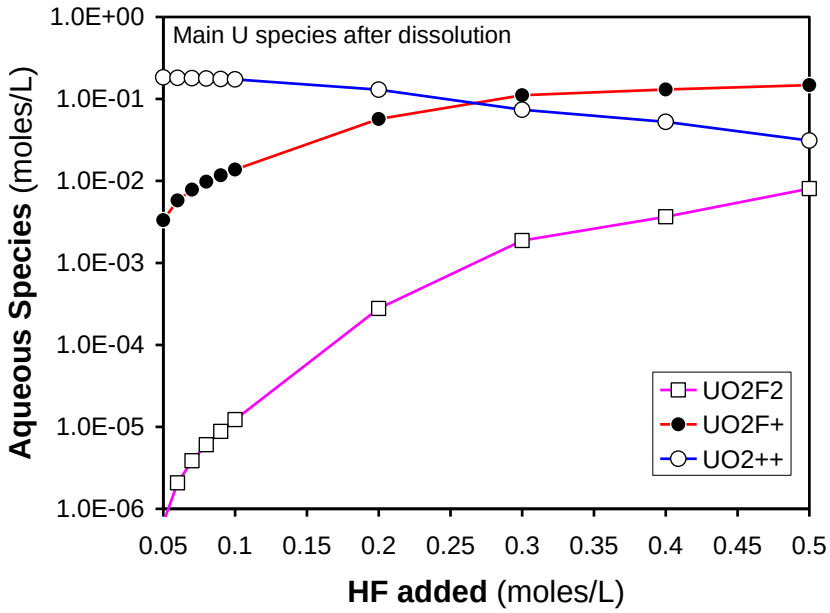

FIGURE 6 (Cont.)

- The dominant iron species present after dissolution are Fe_3^+ and $FeMoO_4^+$. The dominant zirconium species are ZrF^{3+} and ZrF_3^+. The uranyl fluoride complex UO_2F^+ becomes the dominant uranium species at initial HF concentrations greater than 0.3 moles/L.

Figure 6 illustrates dissolver speciation for the dissolution of 50 g/L U-10Mo scrap. Each point represents an equilibrium calculation (full dissolution of metals) for a given initial HF concentration (labeled as HF added). It is assumed that the Al cladding is removed prior to dissolution for the scrap recovery calculations. This model is for the dissolution of 0.21 moles/L U (50 g/L), 0.058 moles/L Mo, and 0.042 moles/L Zr in 3 moles/L HNO_3 containing 0.5 moles/L $Fe(NO_3)_3$ at 25°C. The same model run at 100°C showed similar results.

8.3 MODEL SCENARIO SCRAP (b) (75 g/L U NO Al, TABLE 1, FIGURE 7)

The speciation for the model scenario Scrap (c) (Table 1, Figure 7) is very similar to that described for the Scrap (b) scenario; the main difference is that the Scrap (c) scenario has slightly higher concentrations of uranium, molybdenum, and zirconium.

Figure 7 illustrates dissolver speciation for the dissolution of 75 g/L U-10Mo scrap. Each point represents an equilibrium calculation (full dissolution of metals) for a given initial HF concentration (labeled as HF added). It is assumed that the Al cladding is removed prior to dissolution for the scrap recovery calculations. This model is for the dissolution of 0.31 moles/L U (75g/L), 0.087 moles/L Mo, and 0.063 moles/L Zr in 3 moles/L HNO_3 containing 0.5 moles/L $Fe(NO_3)_3$ at 25°C. The same model run at 100°C showed similar results.

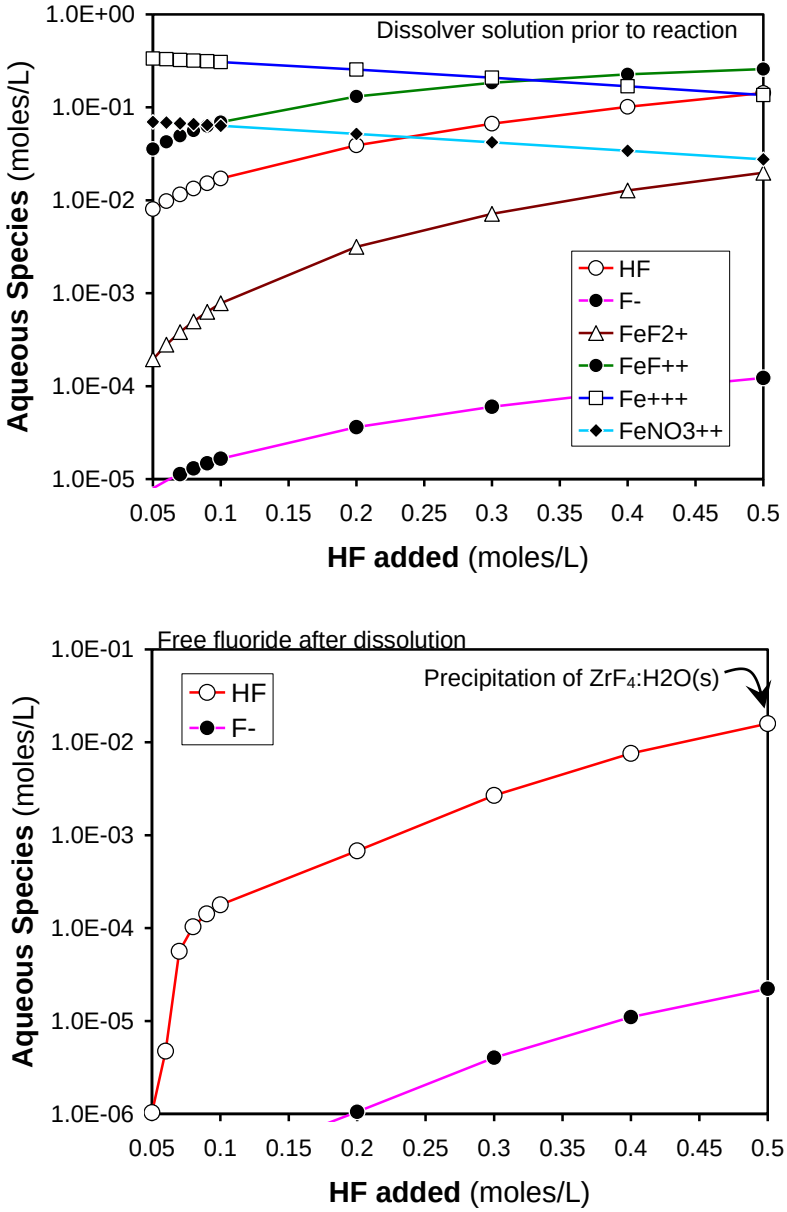

FIGURE 7 Dissolver Speciation for the Dissolution of 75 g/L U-10Mo Scrap (Top: speciation in the dissolver solution prior to reaction with metals. Middle: free fluoride concentration after dissolution of metals. Note the precipitation of a zirconium fluoride solid when the initial HF concentration is greater than 0.45 moles/L. When the model was run at 100°C the zirconium fluoride solid was not predicted to precipitate. Bottom: iron species after dissolution of metals.)

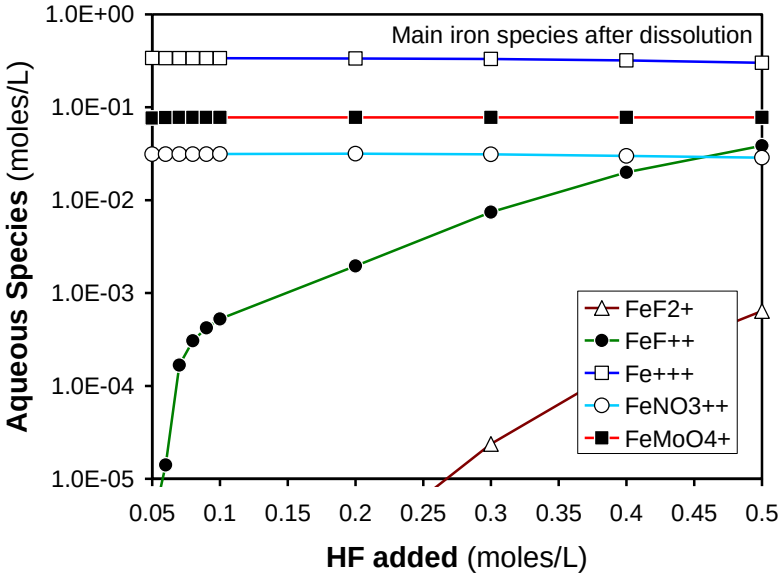

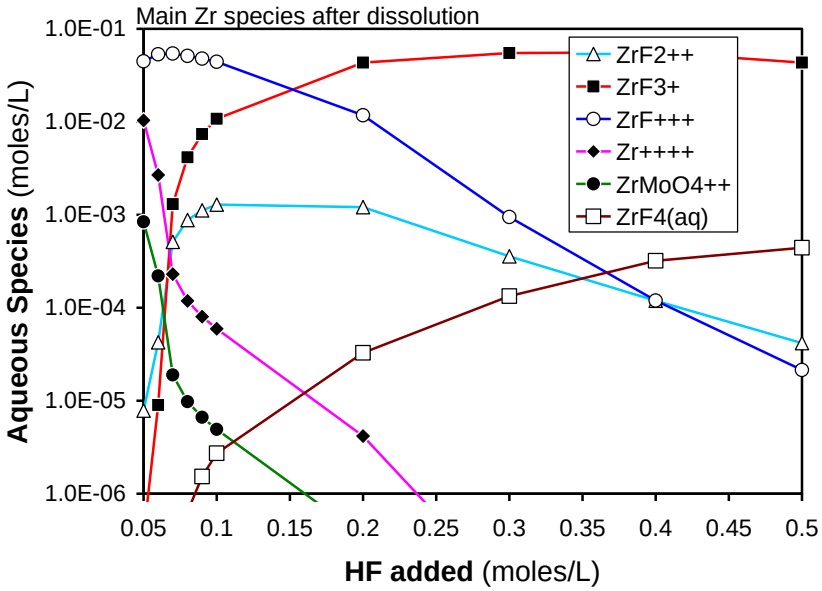

FIGURE 7 (Cont.)

(Plots show zirconium and uranium species in dissolver solution after dissolution of metals as a function of initial HF added.)

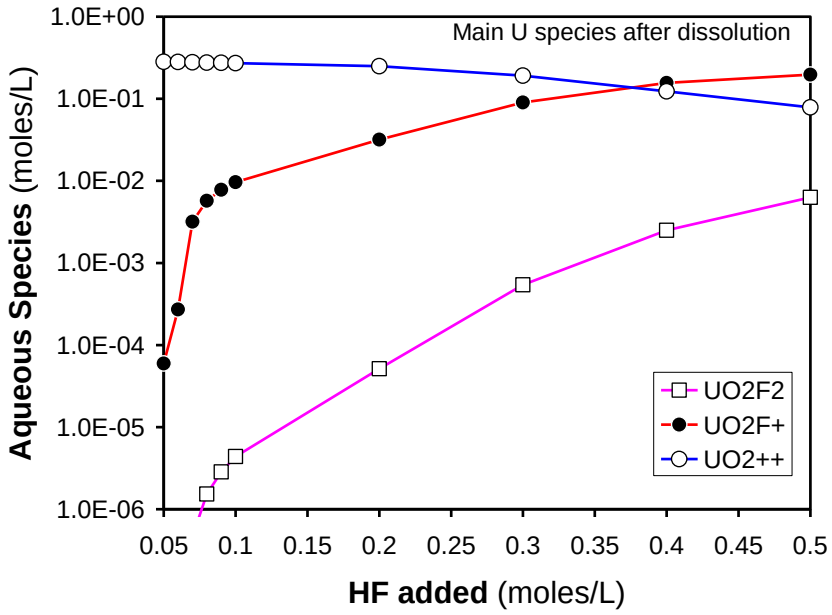

FIGURE 7 (Cont.)

8.4 MODEL SCENARIO SPENT FUEL (a) (20 g/L U WITH Al, TABLE 2, FIGURE 8)

- The free fluoride concentration after the dissolution is 1×10^{-5} to 0.03 moles/L over an initial HF concentration range of 0.1 to 1.0 moles/L HF (the higher initial fluoride relative to the Scrap [a] scenario is due to the presence of the aluminum cladding).

- The model predicts that the dissolver solution will become saturated with respect to the lanthanide fluoride solids (LaF_3 and NdF_3) at initial HF concentrations greater than 0.6 moles/L. At initial HF concentrations greater than 0.9 moles/L, the model predicts that the dissolver solution will be saturated with respect to the aluminum fluoride solid $AlF_3{:}3H_2O$.

- The dominant iron species present after dissolution is iron molybdate ($FeMoO_4^+$). The dominant aluminum species are Al^{3+} at low initial HF concentrations and AlF^{2+} above and initial HF concentration of 0.3 mole/L. The dominant zirconium species are ZrF^{3+} and ZrF_3^+. The zirconium molybdate $ZrMoO_4^{2+}$ is a dominant species at initial HF concentrations less than 0.4 moles/L. The uranyl fluoride complex UO_2F^+ becomes a dominant species at high initial HF concentrations.

- The speciation plots in Figure 8 indicate that an initial HF concentration of at least 0.6 is required to ensure that both aluminum and zirconium are nearly fully complexed as fluoride species, thus mitigating the hazard posed by the

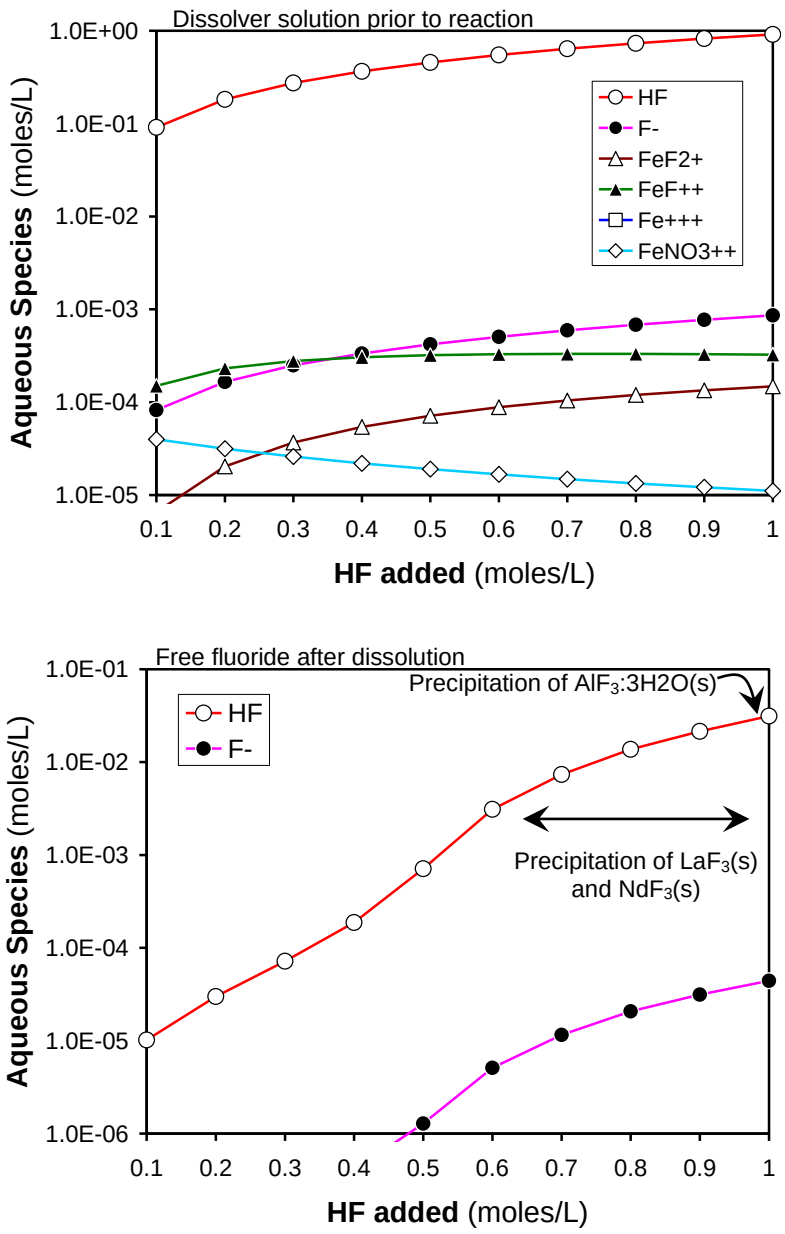

FIGURE 8 Dissolver Speciation for the Dissolution of 20 g/L U-10Mo Spent Fuel (Top: speciation in the dissolver solution prior to reaction with metals. Middle: free fluoride concentration after dissolution of metals. Note the precipitation of a lanthanide fluorides when the initial HF concentration is greater than 0.6 moles/L and the precipitation of aluminum fluoride solid when the initial HF concentration is greater than 0.9 moles/L. When the model was run at 100°C the aluminum fluoride solid was not predicted to precipitate; however, the lanthanide fluorides were predicted to precipitate when the starting HF concentration was greater than 0.6 moles/L. Bottom: iron species after dissolution of metals.)

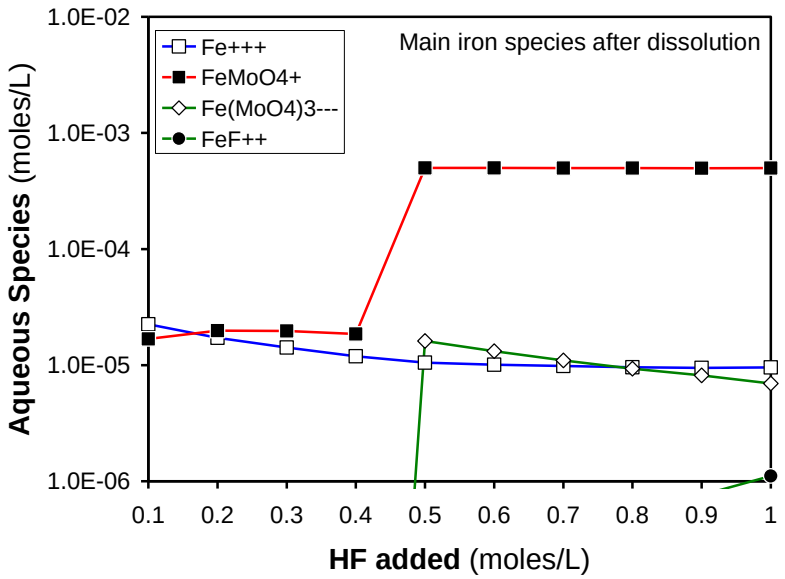

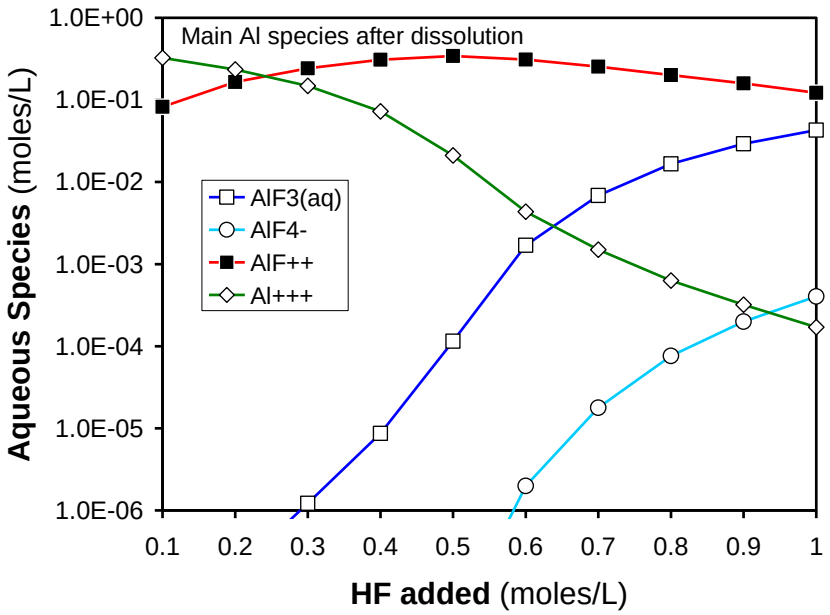

FIGURE 8 (Cont.)
(Plots show aluminum, zirconium, and uranium species in dissolver solution after dissolution of metals as a function of initial HF added.)

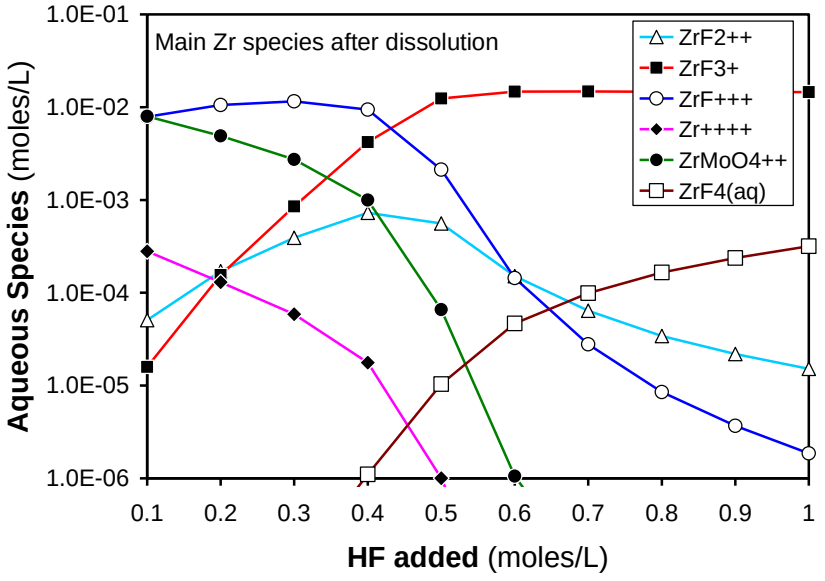

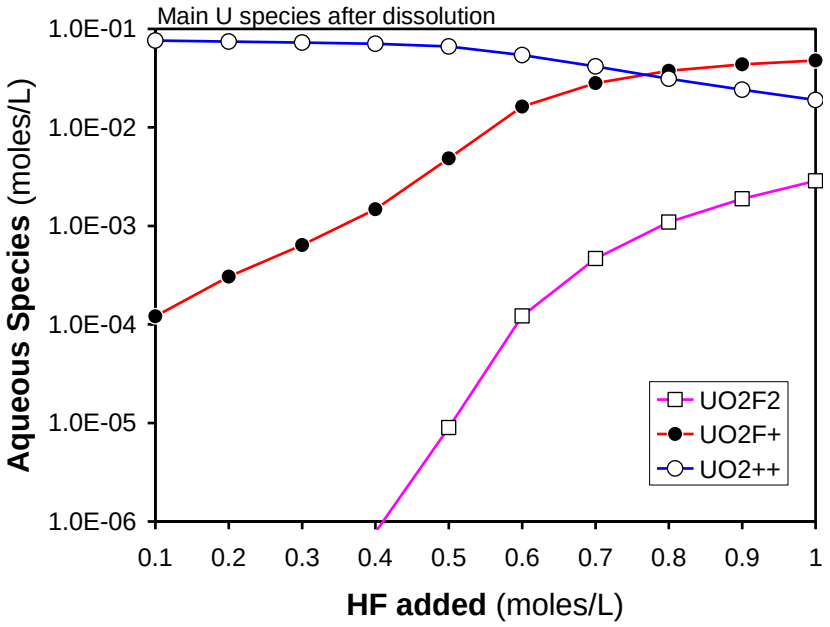

FIGURE 8 (Cont.)

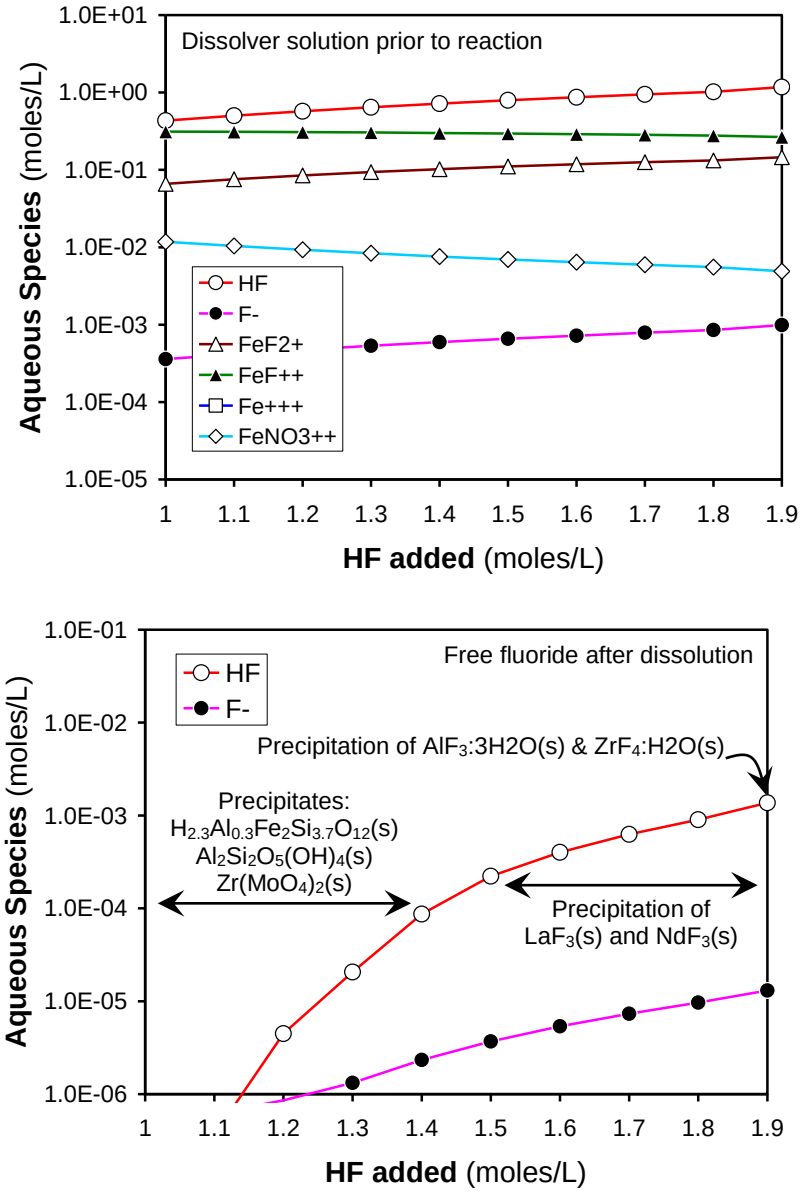

FIGURE 9 Dissolver Speciation for the Dissolution of 50 g/L U-10Mo Spent Fuel (Top: speciation in the dissolver solution prior to reaction with metals. Middle: free fluoride concentration after dissolution of metals. Note the precipitation of a lanthanide fluorides when the initial HF concentration is greater than 0.6 moles/L and the precipitation of aluminum fluoride solid when the initial HF concentration is greater than 0.9 moles/L. When the model was run at 100°C the aluminum fluoride solid was not predicted to precipitate; however, the lanthanide fluorides were predicted to precipitate at when the starting HF concentration was greater than 0.6 moles/L. Bottom: iron species after dissolution of metals.)

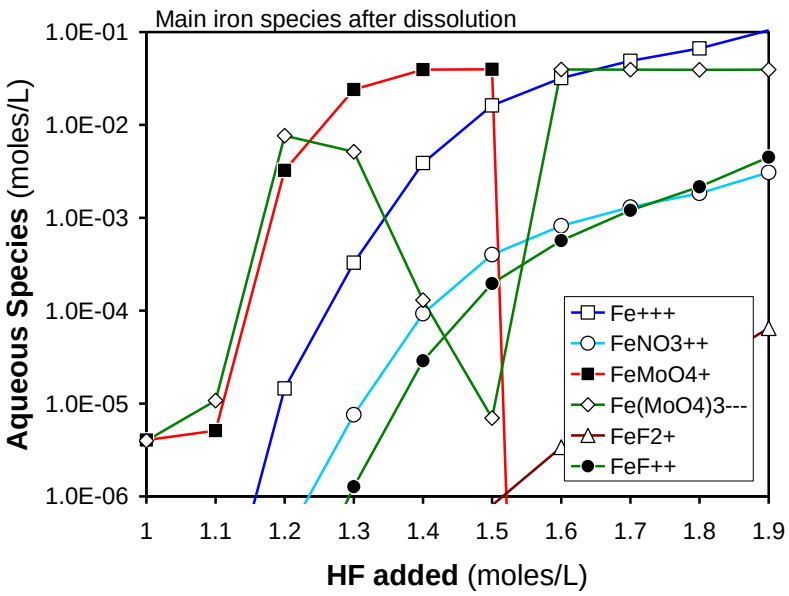

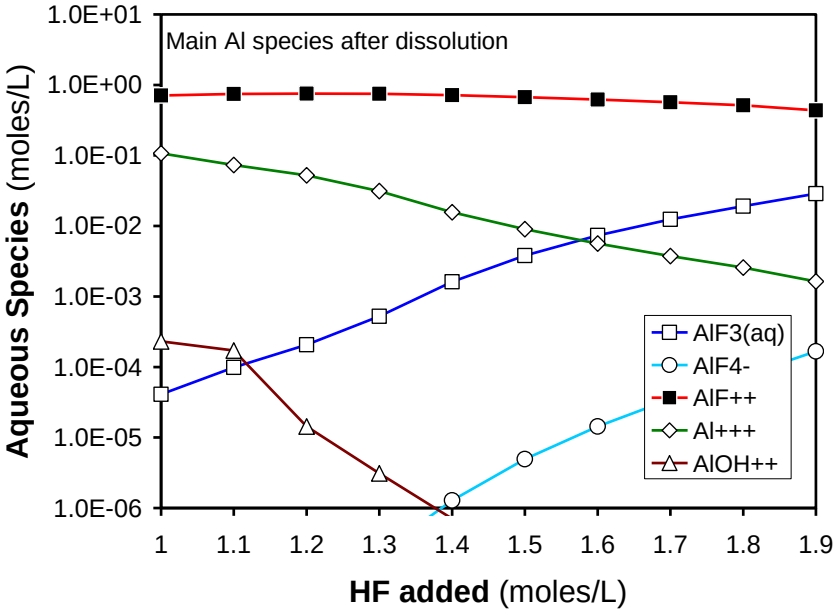

FIGURE 9 (Cont.)
(Plots show aluminum, zirconium, and uranium species in dissolver solution after dissolution of metals as a function of initial HF added.)

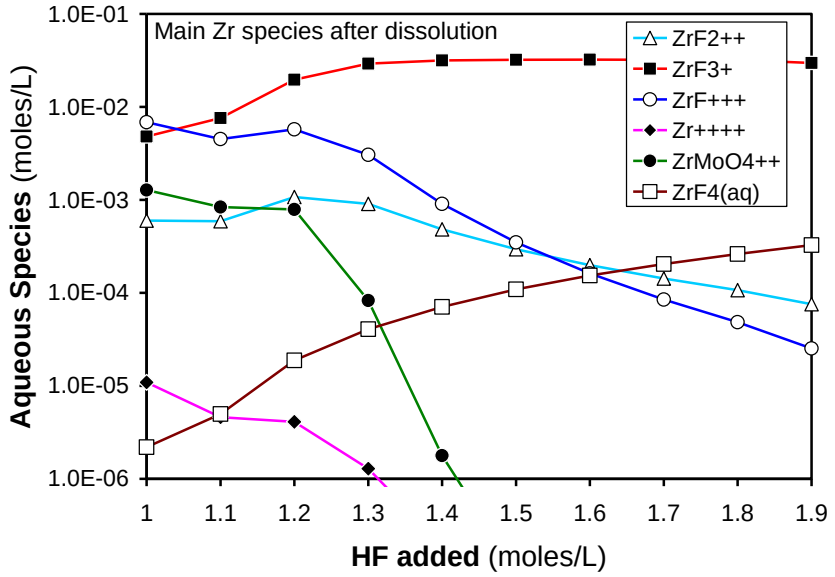

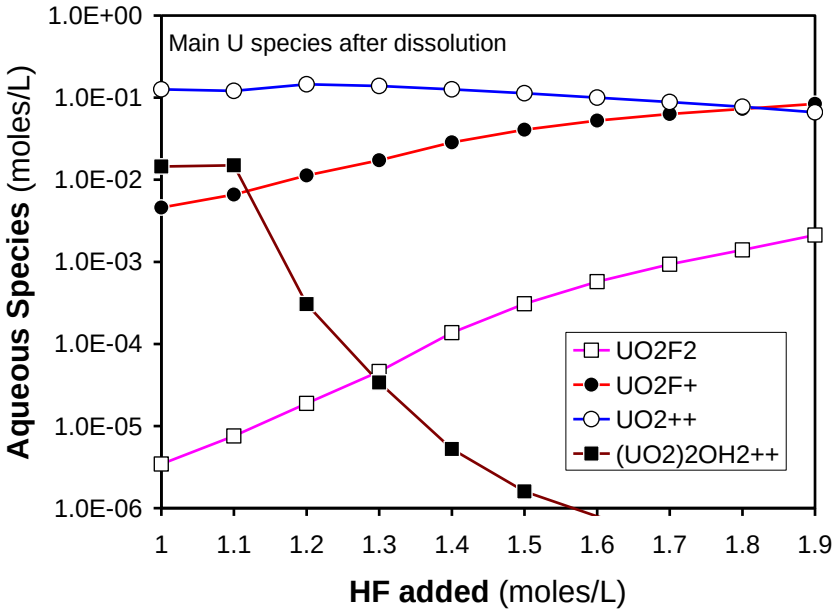

FIGURE 9 (Cont.)

potentially explosive UZr_2 intermetallic phase. This corresponds to a free fluoride concentration of 3.1×10^{-3} moles/L after dissolution. However, the addition of this amount of HF could lead to the precipitation of lanthanide fluoride solids.

Figure 8 illustrates dissolver speciation for the dissolution of 20 g/L U-10Mo spent fuel. Each point represents an equilibrium calculation (full dissolution of metals) for a given initial HF concentration (labeled as HF added). It is assumed that the Al cladding is not removed prior to dissolution of the spent fuel (one-step dissolution). This model is for the dissolution of 0.084 moles/L U (20 g/L), 0.023 moles/L Mo, 0.45 moles/L Al, and 0.017 moles/L Zr in 3 molar HNO_3 containing 6.2×10^{-4} molar $Fe(NO_3)_3$ at 25°C. The same model run at 100°C showed similar results. For fission product concentrations in the spent U-10Mo fuel, see Table 1.

8.5 MODEL SCENARIO SPENT FUEL (b) (50 g/L U WITH Al, TABLE 2, FIGURE 9)

- The free fluoride concentration after the dissolution ranges from less than 1×10^{-6} to 1×10^{-3} moles/L over an initial HF concentration range of 1.0 to 1.9 moles/L HF (the higher initial fluoride relative to the Scrap [b] scenario is due to the presence of the aluminum cladding).

- The low free fluoride concentrations relative to the initial HF added are due to the relatively large mass of aluminum that must be complexed, as well as the precipitation of fluoride solids at initial HF concentrations greater than 1.5 moles/L. The dissolver solution is predicted to become saturated with respect to iron-bearing aluminum silicates and zirconium molybdate at low HF concentrations. At higher initial HF concentrations, the dissolver solution becomes saturated with respect to lanthanide, aluminum, and zirconium fluoride solids.

- The dominant iron species present after dissolution are $Fe(MoO_4)_3^{3-}$ and $FeMoO_4^{+}$. The dominant aluminum species is AlF^{2+} above an initial HF concentration of 0.3 mole/L. The dominant zirconium species are ZrF^{3+} and ZrF_3^{+}. The uranyl fluoride complex UO_2F^{+} becomes a dominant species at high initial HF concentrations.

- The speciation plots in Figure 9 indicate that an initial HF concentration of at least 1.5 moles/L is required to ensure that both aluminum and zirconium are nearly fully complexed as fluoride species, thus mitigating the hazard posed by the potentially explosive UZr_2 intermetallic phase. This corresponds to a free fluoride concentration of 2.2×10^{-4} moles/L after dissolution. However, the addition of this amount of HF could lead to the precipitation of lanthanide fluoride solids.

Figure 9 illustrates dissolver speciation for the dissolution of 50 g/L U-10Mo spent fuel. Each point represents an equilibrium calculation (full dissolution of metals) for a given initial HF concentration (labeled as HF added). It is assumed that the Al cladding is not removed prior to dissolution of the spent fuel (one step dissolution). This model is for the dissolution of 0.21 moles/L U (50g/L), 0.058 moles/L Mo, 1.1 mole/L Al, and 0.042 moles/L Zr in 3 molar HNO_3 containing 0.5 molar $Fe(NO_3)_3$ at 25°C. The same model run at 100°C showed similar results. For fission product concentrations in the spent U-10Mo fuel, see Table 1.

9 CORROSION RATE OF STAINLESS STEEL AND ZIRCONIUM IN THE DISSOLVER SOLUTIONS

In a dissolver solution to which enough HF has been added to mitigate the hazard posed by the potentially explosive intermetallic phase (UZr_2), the free fluoride concentration is approximately 4.0×10^{-3} moles/L for the dissolution of both U-10Mo scrap and spent fuel. However, the amount of HF required for dissolving the U-10Mo spent fuel, such that both the aluminum from the Al-6061 and zirconium are complexed by fluoride, may cause the precipitation of lanthanide, aluminum, and zirconium fluoride solids.

The other constraint on the amount of free fluoride that must be present during the dissolution is determined by the dissolution rate of the aluminum cladding and zirconium bonding layer. The amount of fluoride needed to dissolve the aluminum cladding within a reasonable amount of time (less than 6 hr) is 0.005 moles/L HF. This concentration must be maintained throughout the dissolution process. The amount of fluoride needed to dissolve the zirconium bonding layer within less than an hour is 0.01 moles/L HF (Swanson 1958; Vander Wall et al. 1959); again, this amount must be maintained throughout the dissolution.

In order to safely reprocess aluminum-clad, zirconium-bonded uranium-molybdenum metallic fuel (U-10Mo), a concentration of hydrofluoric acid (HF) must be maintained to dissolve the aluminum cladding and to prevent dangerously rapid reaction of uranium-zirconium intermetallic phases. Existing reprocessing facilities in the United States use fuel dissolvers constructed of 304L stainless steel, and prefer to operate using a single chemical bath. A brief review of literature on the corrosion of 304L stainless steel in nitric acid/HF solution is presented to investigate the feasibility of using these facilities.

The use of HF is not unique to dissolution of fuels containing a U/Zr intermetallic phase. For instance, thoria (ThO_2) fuels require HF for dissolution, and HF has been used with nitric acid for UO_2 fuel reprocessing to accelerate dissolution of difficult to solubilize residues (Ondrejcin and McLaughlin 1980). Some experimental DOE fuels, such as the PuO_2/Al matrix "Mark-42" fuels also require a nitric/hydrofluoric acid mixture (Dunn and Mickalonis 1999; Murray and Crooks 1999). Thus, there is a body of literature we can draw upon to assess the practicality of the proposed approach for reprocessing the aluminum-clad, zirconium-bonded uranium-molybdenum metallic fuel.

Owing to the very similar solution compositions studied, the results of Dunn and Mickalonis (1999) will be the primary focus here, with other literature results presented for comparison. Dunn and Mickalonis (1999) measured corrosion rates of 304 stainless steel coupons in fluorine-containing nitric acid solutions, while monitoring free fluorine using an ion selective electrode. The amount of nitric acid in this study was fixed at 8 M, with fluorine (added as calcium fluoride) varying between 0.2 and 0.5 M. This study also used added aluminum (as metal or aluminum nitrate) at concentrations between 0.2 and 0.5 M, which is fortuitously close to our range of interest for dissolving aluminum-clad U-10Mo. The coupons included both welded and non-welded versions. The use of welded coupons built in a measure of conservatism, as the F-Canyon dissolver is constructed of 304L (rather than standard 304), and the lower

carbon content in 304L minimizes carbide precipitation in the heat-affected zones of the weld region. Carbide precipitates in the weld are more susceptible to intergranular attack. Dunn and Mickalonis (1999) used a constant concentration of 2.2-M boron in all solutions, which would be required for criticality safety when dissolving Pu-containing Mark-42 fuel.

Figure 10 shows the corrosion rate of 304 stainless steel coupons over 1 week of testing from Dunn and Mickalonis (1999). Note that there is substantial variation in corrosion rate depending upon the aluminum concentration; this is because the germane variable is the free fluorine. Rates as high as 248 mils/yr (1 mil = 1/1000 of an inch = ~ 0.0254 mm) have been reported in 10-M nitric acid + 0.01-M HF in solutions with no added complexants, although the rate dropped dramatically with added Zr, Al, or Th (Ondrejcin and McLaughlin 1980). In a proposed thoria/urania dissolver solution consisting of 12-M nitric acid with 0.05-M hydrofluoric acid (initial) plus 0.025-M dissolved zirconium, the corrosion rate of 304L stainless steel was reduced to 13 mils/year (Ondrejcin and McLaughlin 1980). Similar rates (~25 to 100 mils/yr) were observed in the Thorex reprocessing at Oak Ridge (English [1959, 1960], as cited by Cole [1974]). Very high corrosion rates (>>100 mils/yr) are observed for 316 stainless steel in solutions containing only HF with no nitric or available complexants (Osborn et al. 2002)

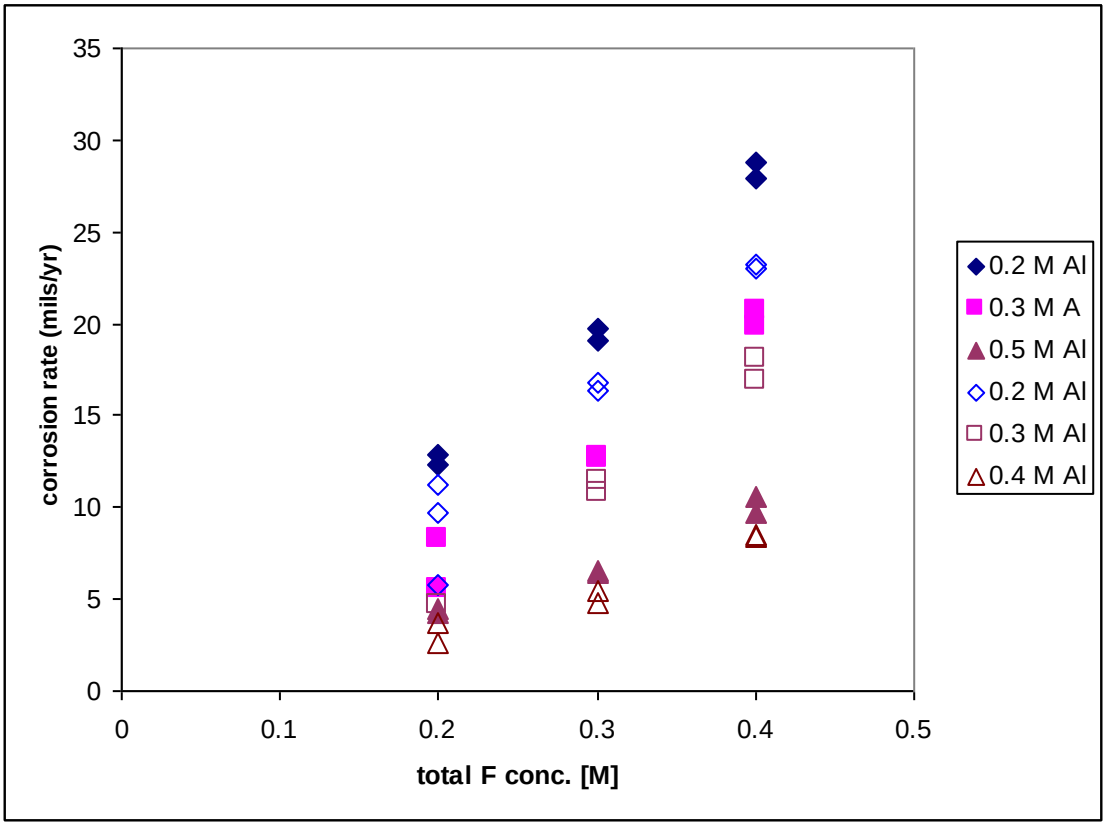

FIGURE 10 Corrosion Rates of 304 Coupons over 1 week of Testing as a Function of Initial Total Fluorine Concentration in 8-M Nitric Acid for Various Concentrations of Added Aluminum (From Dunn and Mickalonis [1999]. Open symbols are single coupons; closed symbols are for welded coupons.)

and for 300-series stainless steels in nitric/HF mixtures containing no complexants (Cole 1974), although the role of complexants in decreasing the corrosion rates, often by orders of magnitude, is acknowledged (Cole 1974). The role of aluminum complexants was studied separately in a brief report by Walker (1957), where 2-M nitric/1 M-hydrofluoric solutions obtained corrosion rates spanning from ~17mils/yr to over 12,000 mils/yr, depending upon the concentration of added aluminum. Although not as widely studied, the corrosion rate in the vapor above the nitric/ hydrofluoric acid solutions has been noted and is generally higher by a factor of less than 3 (Cole 1974).

Although complexants of fluorine clearly play an important role in controlling corrosion rates, there are few reports in the literature of direct measurements of free fluorine concentrations in solutions relevant to our case at hand. Fortunately, the Dunn and Mickalonis (1999) report included such measurements obtained by ion selective electrode. In Figure 11, the corrosion rates of 304 stainless steel coupons are plotted as a function of free fluorine measured at the completion of 1-week tests. Also shown as vertical lines in the plot of Figure 11 are the nominal expected concentrations (or minimal required concentrations) obtained by modeling as discussed earlier in this report. The four labeled scenarios are for scrap [S(a) and S(b)] and irradiated fuels [F(a) and F(b)]. This comparison is more instructive because (1) the variations in corrosion rate now are seen to be more closely an explicit function of free fluorine, rather than aluminum concentration; and (2) the expected corrosion rates for the dissolution scenarios are maintained at less than ~30 mils/yr.

Determination of an “acceptable” rate of vessel corrosion is an empirical task that depends upon the construction of the vessel, the expected time of contact, and the desired service life of the system, among other factors. Such a determination requires an engineering assessment that is beyond the scope of this report, although rates below 50 mpy are considered “low,” “mild,” or “adequate” in similar contexts (Dunn and Mickalonis 1999; Ondrejcin and McLaughlin 1980). Generally, the solution conditions expected compare favorably with prior reprocessing of thoria fuels and Mark-42 fuels, suggesting a tenable operation to reprocess and reclaim aluminum-clad zirconium-bonded U-10Mo fuels with existing facilities.

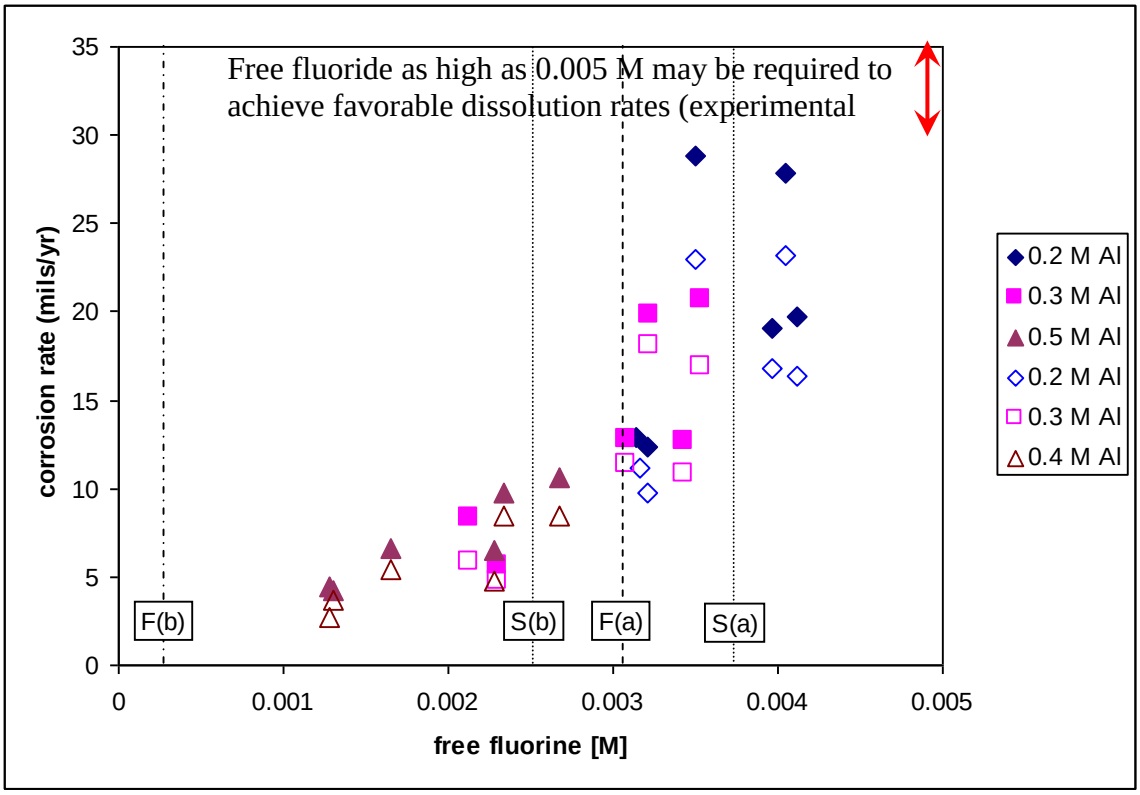

FIGURE 11 Corrosion Rates of 304 Coupons over 1 week of Testing as a Function of Final Free Fluorine Concentration in 8-M Nitric Acid for Various Concentration of Added Aluminum (From Dunn and Mickalonis [1999]. Open symbols are single coupons; closed symbols are for welded coupons. The vertical lines represent final free fluorine concentrations expected for model scenarios Scrap [a] [S(a)], Scrap [b] [S(b)], Fuel [a] [F(a)], and Fuel [b] [F(b)].)

10 CONCLUSION

The dissolution of zirconium- or niobium-bonded U-10Mo fabrication scrap up to 50g/L uranium can be accomplshed safely in 3 moles/L nitric acid, as long as a free fluoride concentration of $>2.6 \times 10^{-3}$ moles/L is maintaned to mitigate the exposive hazard posed by the presence of a uranium-zirconium or uranium-niobium intermetallic phase. Thermodynamic models predict that a possible complication for the scrap dissolution scenarios could be caused by the precipitation of zirconium fluoride at initial HF concentrations greater than 0.5 moles/L.

The dissolution of zirconium or niobium bonded irradiated U-10Mo fuel up to 50g/L uranium can be accomplshed safely in 3 moles/L nitric acid, as long as a free fluoride concentration of $>3.1 \times 10^{-3}$ moles/L is maintaned to mitigate the exposive hazard posed by the presence of a uranium-zirconium or uranium-niobium intermetallic phase. Thermodynamic models predict that the dissolution of irradiated U-10Mo fuel could be complicated by the precipitation of fission product fluorides (lanthanide fluorides), as well as aluminum and zirconium fluorides. The dissolution scenarios for the irradiated fuel assume a one-step process, while the scenarios for the fabrication scrap assume that the aluminum cladding will be removed prior to dissolution.

At the free fluoride concentrations predicted for the scrap and irradiated U-10Mo fuel dissolution scenarios discussed above, the corrosion rate of 304L stainless steel (a potential dissolver vessel material) is predicted to be less than 30 mils/yr. Determination of an "acceptable" rate of vessel corrosion is an empirical task that depends upon the construction of the vessel, the expected time of contact, and the desired service life of the system, among other factors. Such a determination requires an engineering assessment that is beyond the scope of this report, although rates below 50 mpy are considered "low," "mild," or "adequate" in similar contexts. Generally, the solution conditions expected compare favorably with prior reprocessing of thoria fuels and Mark-42 fuels, which suggests a tenable operation to reprocess and reclaim aluminum-clad zirconium-bonded U-10Mo fuels with existing facilities.

Steady-state free fluoride concentrations as high as 0.005 and 0.01 moles/L may be required to achieve favorable aluminum and zirconium dissolution rates (Anderson et al. 1997; Swanson 1958; Vander Wall et al. 1959); however, this constraint needs to be quantified by experimental studies. Aluminum dissolution rates could be improved by addition of $Hg(NO_3)_2$.

11 REFERENCES

Anderson, P.A., and J.D. Christian, 1998, "Alternative Reagent to Mercuric Nitrate Catalyst for Dissolution of Aluminum-Clad Nuclear Fuels in Nitric Acid," *J. Mater. Res.* 13: 68.

Bradford, J.L., and K.L. Adler, 1954, "Pilot-Plant Studies of Mercury-Catalyzed Dissolving of Aluminum-Jacketed Fuel Elements," HW-32316m, U.S. Atomic Energy Commission, July.

Brown P.L, E. Curti, and B. Grambow, 2005, *Chemical Thermodynamics of Zirconium*, Nuclear Energy Agency/OECD, Elsevier, Amsterdam.

Cole, H.S., 1974, *Corrosion of Austenitic Stainless Steel Alloys Due to HNO_3-HF Mixtures*, ICP-1036, Allied Chemical Corporation, Idaho National Engineering Laboratory, October.

Crooks, W.J. III, J.P. Crown, and K.A. Dunn, J.I. Mickalonis, A.M. Murray, and J.D. Navratil, 2003, "Mercury-Free Dissolution of Aluminum-Based Nuclear Material: from Basic Science to the Plant," *Nukleo*. 48: 163.

Dunn, K.A., and J. I. Mickalonis, 1999, *Experimental Study to Evaluate Corrosion of The F-Canyon Dissolver during the Unirradiated Mark-42 Campaign (U)*, WSRC-TR-99-00261, Savannah River Technology Center, August.

Faugeras, P., C. Lheureux, and P. Leroy, 1961, *Etude De Solubilite Du Molybdene en Miliieu Nitrique*, CEA Report No. 1823, Nuclear Study Center, Seclay, France.

Ferris, L.M., 1961a, "Solubility of Molybdic Oxide and Its Hydrates in Nitric Acid, Nitric Acid-Ferric Nitrate and Nitric Acid-Uranyl Nitrate Solutions," *J. Chem. Eng. Data* 6: 600.

Ferris, L.M., 1961b, *Aqueous Processing for Dissolution of Uranium-Molybdenum Alloy Reactor Fuel Elements*, ORNL-3068, Oak Ridge National Laboratory, July.

Gens, T.A., 1958, *Explosive Reactions during Reprocessing of Reactor Fuels Containing Uranium and Zirconium or Niobium*, CF-58-11-31, Oak Ridge National Laboratory, November 13,

Grenthe I., J. Fuger, R.J.M. Konings, R.J. Lemire, A.B. Muller, C. Nguyen-Trung, and H. Wanner, 1992, *Chemical Thermodynamics of Uranium*, Nuclear Energy Agency/OECD, North-Holland/Elsevier, Amsterdam.

Jackson, R.J., and W.L. Johns, 1970, *Explosive Nature of Uranium-base Niobium Alloys after Immersion in Nitric Acid*, RFP-1575, Dow Chemical Company, Rocky Flats Division, December 8.

Larsen, R.P., R.S. Shor, H.M. Feder, and D.S. Flikkema, 1954, *A Study of the Explosive Properties of Uranium-zirconium Alloys*, ANL -5135, Argonne National Laboratory, July.

Moore, G.A., F.J. Rice, N.E. Woolstenhulme, W.D. Swank, C H. DeLon, J.F. Jue, B.H. Park, S.E. Steffler, N.P. Hallinan, M.D. Chapple, and D.E. Burkes, 2008, "Monolithic Fuel Fabrication Process Development at the Idaho National Laboratory," *RERTR 2008 – 30th International Meeting on Reduced Enrichment for Research and Test Reactors*, October 5–9, 2008.

Murray, A.M., and W.J. Crooks III, 1999, *Flow Sheet Development for the Dissolution of Unirradiated Mark 42 Fuel Tubes in F-Canyon Part 11*, WSRC-TR-99-00196, Savannah River Technology Center, June.

Nagarajan K., R. Babu, and C.K. Mathews, 1993, "Enthalpy of Formation of UZr_2 by Calorimetry," *Journal of Nuclear Materials* 203: 221–223.

Ondrejcin, R.S., and B.D. McLaughlin, 1980, C*orrosion of High Ni-Cr Alloys and Type 304L Stainless Steel in HNO_3-HF*, DP-1550, E.I. du Pont Nemours & Co., Savannah River Laboratory, April.

Pierce, R.A., 2007, *Uranium-Molybdenum Dissolution Flowsheet Studies*, WSRC-STI-2007-00103, April.

Schulz, W.W., and E.M. Duke, 1959, *Reprocessing of Low-Enrichment Uranium-Molybdenum Alloy Fuels*, Hanford Atomic Products, HW-62086, September.

Schulz, W.W., R.E. Burns, and E.M. Duke, 1962, "Nitric Acid Dissolution of Uranium-Molybdenum Alloy Reactor Fuels," *Industrial & Engineering Chemistry Process Design and Development* 1: 156.

Stepinski, D.C., J. Swanson, J. Stevens, and G F. Vandegrift, 2008, *Dissolution of U-Mo Alloy Scrap Metal*, Argonne National Laboratory, June.

Swanson, J.L., 1958, "The Zirfelx Process," *Second United Nations International Conference on the Peaceful Uses of Atomic Energy*, June.

Swanson, J.L., 1959, *An Estimation of the Explosion Hazard during Reprocessing of Metallic Uranium Fuel Elements Metallurgically Bonded to Zircaloy Cladding*, HW-62109, Hanford Atomic Products Operation, September 30.

Vander Wall, E.M., and E.M. Whitener, 1959, "Concentrated Nitric and Dilute Hydrofluoric Acid Mixtures in Dissolution of Zirconium Metal," *Ind. Eng. Chem.* 51.

Wachs, D.M., C.R. Clark, and R.J. Dunavant, 2008, *Conceptual Process Description for the Manufacture of Low-Enriched Uranium-Molybdenum Fuel*, Idaho National Laboratory, INL/EXT-08-13840, February.

Walker, W.L., 1957, *Inhibition of HNO_3-HF Corrosion of Type 304-L Stainless Steel with $Al(NO_3)_3 \cdot 9H_20$*, HW-53636, General Electric, Hanford Atomic Products Operation, November 18.

Zeyfang, R.W., 1979, *Hallam Uranium-Molybdenum Fuel Processing*, TA-2-967, September.

Chemical Science and Engineering Division
Argonne National Laboratory
9700 South Cass Avenue, Bldg. 205
Argonne, IL 60439-4837

www.anl.gov

Argonne National Laboratory is a U.S. Department of Energy
laboratory managed by UChicago Argonne, LLC